Imaging Tryptophan Metabolism in Human Brain Tumors

Edit Bosnyák, MD

Ph.D. Thesis

Mentor: Prof. Csaba Juhász, MD, PhD

Co-Mentor: Zoltán Pfund, MD, PhD

Doctoral School Director: Prof. Sámuel Komoly, MD, DSc

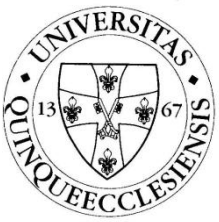

University of Pécs, Medical School, Hungary

Clinical Neuroscience Doctoral Program

Wayne State University, Medical School, Detroit, MI, USA;

PET Center and Translational Imaging Laboratory,

Children's Hospital of Michigan, Detroit, MI, USA

Pécs, 2018

TABLE OF CONTENTS

LIST OF ABBREVIATIONS

AMT: ^{11}C-alpha-methyl-L-tryptophan

AUC: area under the curve

BDI-II: Beck Depression Inventory, 2nd Edition

CBTRUS: Central Brain Tumor Registry of the United States

CNS: central nervous system

DWI: diffusion-weighted imaging

EGFR: epidermal growth factor receptor

FDG: 2-deoxy-2[^{18}F]fluoro-D-glucose

FDOPA: ^{18}F-fluoro-L-dihydroxy-phenylalanine

FET: ^{18}F-fluoroethyl-tyrosine

FLAIR: fluid-attenuated inversion recovery

FWHM: full-width half-maximum

GBM: glioblastoma

HR: hazard ratio

IDH: isocitrate dehydrogenase

IDO: indoleamine 2,3-dioxygenase

iRANO: immunotherapy-RANO

KMO: kynurenine 3-monooxygenase

KP: kynurenine pathway

KPS: Karnofsky Performance Status

KYNU: kynureninase

LAT: L-type amino acid transporter

MET: L-[methyl-^{11}C]methionine

MGMT: O^6-methylguanine–DNA methyltransferase

MPRAGE: magnetization-prepared rapid gradient-echo

MRI: magnetic resonance imaging

MRS: MR spectroscopy

NAA: N-acetylaspartate

NSCLC: non-small cell lung cancer

PET: positron emission tomography

PWI: perfusion-weighted imaging

RANO: Response Assessment in Neuro-Oncology

ROC: receiver-operating characteristics

ROI: region of interest

RPA: Recursive Partitioning Analysis

SUV: standardized uptake value

TDO: tryptophan 2,3-dioxygenase

TERT: telomerase reverse transcriptase

T1-Gad: post-contrast T1-weighted

TTFields: tumor-treating fields

VD: volume of distribution

VEGF: vascular endothelial growth factor

VOI: volume of interest

WHO: World Health Organization

I. INTRODUCTION

I.1. Epidemiology of brain tumors

Brain tumors are relatively rare cancer types in adults but represent the most common solid tumors in children. In all ages, brain tumors carry a significant mortality, and, therefore, are considered to be a major health care issue. The majority of newly-diagnosed brain masses are metastatic tumors, while the rest represent a variety of primary central nervous system (CNS) tumors. According to the 2016 Central Brain Tumor Registry of the United States (CBTRUS) report, the overall incidence rate of all primary CNS tumors is 22.36/100,000 in the United States [Ostrom et al., 2016]. The worldwide incidence rate of malignant primary CNS tumors in 2012 was 3.4/100,000 [Ostrom et al., 2016]. The annual average mortality rate related to primary malignant CNS tumors between 2009-2013 in the United States was 4.32/100,000 and an estimated 16,947 deaths will be related to primary CNS tumors in 2017 [Ostrom et al., 2016]. Based on the Austrian Brain Tumor Registry, the number of primary brain tumors was 1,688 in a population of 8.2 million in 2005 (18.1/100,000/year) [Wöhrer et al., 2009]. The incidence rate was higher in females than in males, and the most common primary brain tumor was meningioma and also the most common of all non-malignant tumors (53,2%). However the most common of all malignant CNS tumors was glioblastoma (46,6%) [Ostrom et al., 2016].

There are a few known risk factors associated with brain tumors, such as ionizing radiation and genetic predisposition. The most common radiation-induced tumors are gliomas, meningiomas and schwannomas [Fisher et al., 2007]. Oxidative stress, that may impact the pathogenesis of migraine-related white matter lesions by influencing cerebrovascular

autoregulation and vasomotor reactivity, also has a role in gliomagenesis by increased intracellular reactive oxygen species (ROS) [Rinaldi et al., 2016]. Genetic susceptibility for brain tumors may exist, however, the majority of brain tumors are sporadic [McNeill, 2016]. On the other hand, autoimmune conditions and allergies are inversely correlated with glioma risk [Brenner et al., 2002; Wiemels et al., 2002; Schoemaker et al., 2006; Schwartzbaum et al., 2003].

Among various types of primary CNS tumors, meningioma is the most frequently reported histology overall (36.6%), followed by pituitary tumors (24.1%), and glioblastoma (14.9%) [Ostrom et al., 2016]. In pediatric populations (ages 0-14 years), brain and other CNS tumors are the most common solid tumors and the cause of the majority of cancer mortality [de Blank PM et al., 2015]. The most common brain tumors in children are pilocytic astrocytoma and medulloblastoma [McNeill, 2016]. In adolescent and young adult populations (ages 15-39 years), the incidence rate of primary CNS tumors is 10.71/100,000 and higher for non-malignant than malignant tumors.

In the adult population above age 40 years, the average annual age-adjusted incidence rate of primary CNS tumors is 40.10/100,000. The 5-year relative survival of primary malignant CNS tumors between 1995-2013 was 34.7% (higher in females), but it was modified significantly by age, histology and clinical behavior, while in non-malignant CNS tumors, 5-year survival was 90.4% in the United States [Surveillance Epidemiology and End Results (SEER) Program, 2016].

I.2. Clinical manifestation of brain tumors

In general, the most common clinical manifestations of brain tumors include seizure, focal neurological deficit, altered behavior, and cognitive impairment, but mood disturbance and depression are also common co-morbidities among these patients [Rooney et al., 2011; Goebel et al., 2013].

In gliomas, the age of the patients and also tumor grade have a significant effect on the presenting symptoms [Posti et al., 2015]. Seizure can be a common symptom in patients with low-grade glioma (approximately 80%) [Pallud et al., 2010; Ruda et al., 2010; Ruda et al., 2012] and also in patients with a younger age [Ruda et al., 2012], while in patients with anaplastic astrocytoma and glioblastoma, the most common manifestations are focal neurological deficit (such as signs of high intracranial pressure, headache, paresis) and cognitive deficit [Riva et al., 2006; Tanaka et al., 2012]. However, in some cases, the only manifestation of brain tumors is different psychiatric symptoms, such as depression, apathy, personality changes, anxiety, etc. [Madhusoodanan et al., 2015]. Most epidemiologic data related to brain tumor-associated depression have encompassed primarily glioma patients, where the estimated prevalence of depression ranges from 6 to 93 % [Rooney et al., 2011]. While depression in brain tumor patients is an important component of the quality of life, and, possibly, survival [Rooney et al., 2011; Mainio et al., 2005; Pelletier et al., 2002], many patients are neither properly diagnosed nor adequately treated for depression. Effective treatments include antidepressants (such as serotonin reuptake inhibitors) and psychotherapy.

Meningiomas are mainly solitary tumors [Claus et al., 2005], and approximately 2-3 % of the population has an incidental asymptomatic meningioma [Porter et al., 2010]. One of the most common manifestation of meningiomas is seizure, which occurs in 13-60% of affected patients and is among the initial symptom in 20-50% of them [Hamasaki et al., 2012; Lieu et al., 2000]. Studies reported that 53-90% of patients with preoperative seizures can be seizure-free after tumor resection [Gonzales-Martinez et al., 2008; Hamasaki et al., 2012; Lieu et al., 2000].

I.3. Classification of brain tumors

Until the recent revision in 2016, the classification of CNS tumors mainly relied on conventional histopathologic characteristics [Louis et al., 2007]. However, in the recently released 2016 World Health Organization (WHO) classification of CNS tumors, for the first time, molecular markers have been incorporated in addition to conventional histology to classify primary brain tumors, thus formulating a new concept as to how CNS tumor diagnoses should be established using recently recognized molecular characteristics [Louis et al., 2016]. This classification also added some newly recognized neoplasms and deleted some others that have no longer diagnostic and/or biological relevance (e.g., the use of oligoastrocytoma as a separate entity is now discouraged, because astrocytomas and oligodendrogliomas can be distinguished by specific molecular markers). Other changes included the addition of brain invasion as a criterion for atypical meningioma and the introduction of a soft tissue-type grading system [Louis et al., 2016]. In the future, the 2016 WHO classification might be helpful to faciliatet improved diagnostic accuracy, more personalized and targeted patient management, as well as reliable determination of the prognosis and treatment response.

I.4. Common brain tumor types in adults

I.4.1. Gliomas. Gliomas are a heterogeneous group of CNS tumors, derived from neuroglial progenitor cells. Gliomas represent approximately 27% of all primary brain tumors and 80% of malignant primary brain tumors [Ostrom et al., 2015]. The cause of glioma is still unknown, but ionizing radiation is a known risk factor, as well as genetic predisposition (increased risk of glioma in rare familiar tumor syndromes, such as neurofibromatosis type 1 and 2, Li Fraumeni syndrome, Turcot syndrome).

Gliomas can be distinguished as oligodendrogliomas, astrocytomas and ependymomas based on histology and WHO grade I-IV depending on tumor malignancy (increasing aggressiveness with higher grade). Grade I and II (diffuse infiltrating gliomas) are low-grade gliomas, while grade III (anaplastic gliomas) and grade IV (glioblastomas) are high-grade gliomas. Low-grade gliomas occur more commonly in young adults (30-45 years), while grade III anaplastic glioma occurs around 45 years of age and glioblastoma (GBM) around 60 years of age, on average. Based on the new 2016 WHO classification of CNS tumors, nearly all of gliomas can be classified either as astrocytoma or oligodendroglioma [Sahm et al., 2014; Cancer Genome Atlas Research Network, 2015; Wiestler et al., 2014; Louis et al., 2016] (**Table 1., see next page**). Diagnosis of oligoastrocytomas should be confined to cases with an inconclusive genetic test or absence of an appropriate molecular test. In addition, one genetically defined subtype (ependymoma, RELA-fusion positive) has been accepted. This variant represents the majority of supratentorial tumors in the pediatric population [Louis et al., 2016].

Table 1. 2016 WHO Classification of CNS tumors - Gliomas

2016 WHO Classification of Gliomas				
Diffuse astrocytic and oligodendroglial tumors		**Grade**	**Other astrocytic tumors**	**Grade**
Diffuse astrocytoma	IDH mutant	II	Pilocytic astrocytoma	I
Gemistocytic astrocytoma	IDH mutant		*Pilomyxoid astrocytoma*	
Diffuse astrocytoma	IDH wild-type		Subependymal giant cell astrocytoma	I
Diffuse astrocytoma	NOS		Pleomorphic xanthoastrocytoma	II
			Anaplastic pleomorphic xanthoastrocytoma	III
Anaplastic astrocytoma	IDH mutant	III		
Anaplastic astrocytoma	IDH wild-type		**Ependymal tumors**	
Anaplastic astrocytoma	NOS		Subependymoma	I
			Myxopapillary ependymoma	I
Glioblastoma	IDH mutant	IV	Ependymoma	II
Glioblastoma	IDH wild-type	IV	*Papillary ependymoma*	
Giant cell glioblastoma			*Clear cell ependymoma*	
Gliosarcoma			*Tanycytic ependymoma*	
Epitheloid glioblastoma			Ependymoma, RELA fusion-positive	II or III
Glioblastoma	NOS		Anaplastic ependymoma	III
Diffuse midline glioma	H3 K27M-mutant	IV	**Other gliomas**	
			Chordoid glioma of the third ventricle	II
Oligodendroglioma	IDH mutant and 1p/19q co-deleted	II	Angiocentric glioma	I
			Astroblastoma	
Oligodendroglioma	NOS			
			Mixed neuronal-glial tumors	
Anaplastic Oligodendroglioma	IDH mutant and 1p/19q co-deleted	III	Ganglioglioma	I
			Analpastic Ganglioglioma	III
Anaplastic Oligodendroglioma	NOS		Desmoplastic infantile astrocytoma	I
			Desmoplastic infantile ganglioglioma	I
Oligoastrocytoma	NOS	II	Papillary glioneuronal tumor	I
Anaplastic oligoastrocytoma	NOS	III	Rosette-forming glioneuronal tumor	I
			Diffuse leptomeningeal glioneuronal tumor*	

IDH: isocitrate dehydrogenase; NOS: not otherwised specified

Cells with new entities shaded with grey color

* definitive WHO Grade has not yet been assigned

Estimated survival of gliomas is different depending on tumor histology; 5-year survival rate for pilocytic astrocytoma is 94.2%, while it is only 5.5% for glioblastoma [Ostrom et al., 2016]. The oligodendroglial subtype has a better prognosis (10-15 years median survival) than the astrocytic subtype (6 years median survival) [Pignatti et al., 2002].

Glioblastoma (WHO Grade IV astrocytoma) is the most common form of gliomas and the most common primary brain tumor in adults after meningiomas [Ostrom et al., 2014], representing approximately 45% of malignant primary brain tumors and about 15% of all primary brain tumors [Louis et al., 2007; Ostrom et al., 2013] with 14-16 months overall median survival [Stupp et al., 2009; Omuro et al., 2013]. About 90% of glioblastomas are primary with an older median age at time of diagnosis (~64 years), and the remaining 10% are secondary developing from low-grade diffuse astrocytoma or oligodendroglioma typically at a younger age [Wen & Kesari, 2008].

I.4.1.1. Histopathology and prognostic biomarkers in malignant gliomas

Accurate histopathological diagnosis is very important for prognosis and treatment of brain tumors. The most important histopathologic features of glioblastomas include significant necrosis, microvascular proliferation, high mitotic activity, nuclear atypia, high cellularity and also "pseudopalisading" [Agnihotri et al., 2013]. However, the differentiation between tumor grades may be challenging. Assessment of mitotic activity plays an essential role in tumor grading, and Ki-67 nuclear labeling index became a commonly used prognostic and diagnostic marker to estimate tumor proliferative activity. Ki-67/MIB-1 proliferative index showed a positive correlation with histological malignancy grade in all gliomas, but it also showed overlap between the malignancy

subgroups [Skjulsvik et al., 2014]. Based on this finding, Ki-67 is useful but alone not sufficient to determine precisely the malignancy grade.

It has been increasingly recognized that there are key genetic tumor markers affecting prognosis and treatment response (**Table 2.**). Analysis of The Cancer Genome Atlas identified more than 60 genetic alterations including genetic mutations and chromosomal aberrations in glioblastoma [Cancer Genome Atlas, 2008; Parsons et al., 2008; Belden et al., 2011]. A number of prognostic and predictive genetic glioma biomarkers have emerged during the last decade. Prognostic biomarkers provide information about the length of survival regardless of treatment [Simon, 2010; Tezak et al., 2010]. Predictive biomarkers compare the effect of certain therapy in patients with and without biomarkers and could differentiate the effect of this treatment on the outcome. Main prognostic factors for gliomas include age, clinical performance status (commonly evaluated by the Karnofsky Performance Status (KPS) Scale [Schag et al., 1984]), and extent of initial resection. In addition, several specific molecular biomarkers have important prognostic or predictive significance in malignant gliomas [Wilson et al., 2014] (**Table 2.**), as detailed in the upcoming section.

Table 2. Most important genetic molecular biomarkers in gliomas

Glioma biomarker	Effect	Survival
IDH1 mutation	Common in secondary GBM (85%). Younger patient population. No cellular protection against oxidative damage.	better
1p/19q deletion	Independent prognostic biomarker. GBM with oligodendroglial component. Favorable response to chemo- and radiotherapy.	better
MGMT promoter methylation	32-68% of primary GBM. 75% of secondary GBM. Predictor of response to alkylating agent.	better
EGFR overexpression	Augmentation of tumor angiogenesis, cell proliferation, cell survival.	worse
TP53 mutation	Mainly in secondary GBM (62%), diffuse and anaplastic astrocytomas. Strong association with IDH1 mutation in diffuse astrocytomas.	worse
TERT mutation	TERT upregulation and survival of tumor cells.	worse

The most significant GBM genetic biomarkers include isocitrate dehydrogenase-1 (IDH1) mutation, 1p/19q co-deletion (GBM with oligodendroglial component, 4.2/27.2 %), O^6-methylguanine–DNA methyltransferase (MGMT) promoter methylation, epidermal growth factor receptor (EGFR) overexpression (approximately in 50% of GBM) and TP53 mutation (**Table 2.**). Based on the presence of IDH1 mutation, GBMs can be separated into two subgroups: IDH1 wild-type or primary glioblastoma, which are more likely to carry EGFR amplification, occur in older population, and have a worse prognosis; while IDH1 mutated (secondary) glioblastomas are more likely to carry TP53 mutation, occur in younger population, and have a better prognosis [Appin et al., 2014].

In addition, several studies reported a significant association between human telomerase reverse transcriptase (TERT) mutation and gliomas. Telomer length is an important mechanism involved in the immortalization of cancer cells. TERT mutation presents frequently in glioblastomas (69%) and oligodendrogliomas (72%), but it is less common in astrocytomas (38%) [Yuan et al., 2016]. Also gliomas with only TERT mutation are primary GBMs, associated with poor overall survival, while secondary GBMs have a low frequency of TERT promoter mutations [Eckel-Passow et al., 2015; Yuan et al., 2016]. Based on the developing genetic profile of glioblastomas, Verhaak et al. [2010] classified 4 different molecular subgroups of GBMs, such as proneural, neural, classical and mesenchymal. Patients with classical and mesenhcymal GBM subtypes showed significantly better survival with the use of concurrent temozolomide, while the survival was not changed in the proneural subtype. IDH1 mutations were mostly found in proneural gliomas, while NF1 alteration was associated with mesenchymal subtype and EGFR alterations were associated with classical subtype [Wang et al., 2016]. They also reported that 75% of primary GBMs switched transcriptional subtype at relapse, whereas secondary GBMs were more stable.

I.4.1.2. Treatment options and prognosis of malignant gliomas

Current standard treatment for glioblastoma includes surgical resection (gross total or partial tumor resection) followed by radiotherapy and concurrent systemic chemotherapy with temozolomide ("Stupp regimen") [Stupp et al., 2005]. A phase III clinical trial showed that temozolomide added during (75 mg/m^2 per day) and after (150-200 mg/m^2, 5 days every 28 days for six cycles) standard radiotherapy (60 Gy to the tumor) has a

positive effect on median overall survival (14.6 vs. 12.1 months) and the 2-5-year survival rate, compared with radiotherapy alone [Stupp et al., 2005; 2009]. During the initial 2-3 months of treatment, 20-30% of patients show clinical deterioration ("pseudoprogression") and apparent MRI progression due to therapy-related injury to the blood-brain barrier [Brandsma et al., 2008]. Based on this, in patients who have clinically asymptomatic progressive lesion after the end of chemoradiotherapy with temozolomide, adjuvant temozolomide should be continued [Brandsma et al., 2008]. However, if the early progression is not definitely "pseudoprogression", biopsy might be indicated. In recurrent glioblastoma management, re-resection can be offered in selected cases; also the patients can be enrolled in an ongoing clinical trial.

Other, novel therapies of glioblastomas are also being investigated. These include molecularly targeted therapies (including inhibition of angiogenesis pathways by vascular endothelial growth factor (VEGF) ligand blocker bevacizumab), immunotherapy and gene therapy [Delgado-Lopez et al., 2016]. Studies have shown a high response rate (30-50%) to bevacizumab given alone or in combination with irinotecan, associated with 35-50% estimated 6-month progression-free survival in patients with recurrent tumor [Friedman et al., 2009; Vredenburgh et al., 2007; Kreisl et al., 2009]; however, two phase III clinical trials failed to show an overall survival benefit from bevacizumab treatment [AVAGlio trial and RTOG-0825 trial, Weller & Yung, 2013**]**. Recently, a new treatment modality, Tumor-Treating Fields (TTFields) administered through an alternating electric field device (NovoTTF-100A or Optune), aimed to disrupt tumor cell division, has been presented as a promising new tool for delaying progression of glioblastoma [Kirson et al., 2004; 2007; 2009; Stupp et al., 2012; 2015]. In patients with recurrent disease, TTFields

therapy proved to be as efficacious as temozolomide without its systemic side effects [Stupp et al., 2012; Bosnyák et al., 2017; Mittal et al., 2017]. In a recent study, TTFields combined with temozolomide, utilized as upfront therapy in newly diagnosed glioblastoma, provided a 4-month survival benefit as compared to temozolomide alone [Stupp et al., 2015]. Combined TTFields therapy and bevacizumab is still under investigation [Delgado-López & Corrales-García, 2016].

I.4.2. Meningiomas. Meningiomas are the most common primary CNS tumors in adults. Meningioma incidence increases with age, and these tumors occur about twice as often in women as in men. Meningiomas are mostly benign and slowly growing [Ostrom et al., 2013], but they also could recur and progress into a malignant form [Louis et al., 2007].

Meningiomas have 13 histological subtypes and three grades of malignancy [Perry et al., 2007]. The overall classification of meningiomas and also the grading did not undergo any recent revision. The most important predictor of the recurrence risk in meningiomas is the WHO histological grade, which is based on the local invasiveness and cellular features of atypia [Louis et al., 2007]. In the 2016 WHO classification, brain invasion joins the mitotic count of 4 or more as a histological criterion that can be enough for diagnosing an atypical meningioma, WHO grade II. Approximately 70-80% of meningiomas are grade I with 9 histological subtypes, from which meningothelial, fibrous and transitional are the most common. Grade II tumors represent up to 20% of all meningiomas and include 3 subtypes, atypical, chordoid and clear-cell variant. Finally, grade III accounts for 1-28% of meningiomas and include papillary, rhabdoid and anaplastic forms [Perry et al., 2007; also see **Table 3**.].

Table 3. 2016 WHO Classification of CNS tumors - Meningiomas

2016 WHO classification of meningiomas	
Subtypes of Meningioma	**Grade**
Meningothelial meningioma	I
Fibrous meningioma	I
Transitional meningioma	I
Psammomatous meningioma	I
Angiomatous meningioma	I
Microcystic meningioma	I
Secretory meningioma	I
Lympholasmacyte-rich meningioma	I
Metaplastic meningioma	I
Brain invasive	II
Chordoid meningioma	II
Clear cell meningioma	II
Atypical meningioma	II
Papillary meningioma	III
Rhabdoid meningioma	III
Anaplastic (malignant) meningioma	III

However, a recent study reported that in the WHO classification, concordance in the histological grading of meningiomas is still suboptimal [Rogers et al., 2016], especially in the diagnosis of grade II meningiomas. Biomolecular markers also have a role in grading: different histological types have different molecular alterations [Bi et al., 2016], and subgroups can be defined based on their genetic profile [Brastianos et al., 2013; Lee et al., 2010]. TERT promoter mutations are associated with meningiomas with higher grade and also with those with higher risk for recurrence and progression [Koelsche et al., 2013; Goutagny et al., 2014; Sahm et al., 2015]. This mutation seems to be superior to

histological grade to predict recurrence-free survival [Sahm et al., 2015], and it might be useful to establish the progression risk of meningiomas. In addition, the presence of progesterone receptor is more frequent in benign meningioma and associated with better prognosis, while the expression level of VEGF was greater in atypical and anaplastic meningiomas predictive for higher risk of recurrence. Deletion of 14q was an independent prognostic marker for tumor recurrence [Saraf et al., 2011].

Initial treatment of meningiomas is gross total surgical resection including the involved dura [Goldbrunner et al., 2016]. The extent of resection, defined by the *Simpson grade (Grade I-V)* [Simpson, 1957], remains an important prognostic factor of recurrence risk even today [Winther & Torp, 2016]. As an alternative treatment, stereotactic radiosurgery can be done for small tumors or fractionated radiotherapy for larger or previously treated meningiomas. Also, if the complete resection of the tumor is not possible, external-beam radiation or partial resection with adjuvant chemotherapy are options [Saraf et al., 2011]. However, in elderly patients or asymptomatic, incidentally discovered meningiomas, observation (watchful waiting) is also a reasonable therapeutic option. Radiation therapy is frequently recommended after surgery for high-grade meningiomas, although it may not be completely efficacious. Chemotherapeutic options still remain very limited. The 5-year recurrence rate after surgery is 12% for grade I, 41% for grade II, and 56% for grade III meningioma. In grade I meningiomas, MRI follow-up is recommended annually for 5 years, and every two years afterwards. In grade II tumors, imaging is recommended at 6 months, then annually, while in grade III, MRI should be done every 3-6 months [Goldbrunner et al., 2016].

I.4.3. Brain metastases. Brain metastases are the most common intracranial tumors in adults. Although the exact prevalence of brain metastases is unknown, they may occur approximately in 20-40% of patients with cancer [Arnold & Patchell, 2001; Soffietti et al., 2002]; however, at the time of the diagnosis, in 8-15% of the patients, the primary tumor is unknown (CUP: cancer of unknown primary) [Bartelt & Lutterbach, 2003]. Lung and breast cancer as well as melanoma are the most common cancer types to develop brain metastases, while metastases from kidney, colorectal region, prostate, testis and ovary are less frequent [Soffietti et al., 2002; Schouten et al., 2002]. Mean overall survival has been dismal, although the majority of the patients survive at least 6 months after the diagnosis [Sperduto et al., 2012]. Early detection of metastatic brain tumors, when only a single or few lesions are present, may allow focal therapy, such as tumor resection or stereotactic radiosurgery. The main goal of the treatment is improving quality of life by palliating symptoms [Hall et al., 2000; Wong et al., 2008]. The recent therapeutic options include surgery, stereotactic radiosurgery (SRS), whole brain radiotherapy (WBRT), systemic therapy and palliative therapy only. Corticosteroids can alleviate symptoms of brain metastases, such as edema and neurological symptoms of increased intracranial pressure; however, treatment with corticosteroids alone is indicative of poor survival **[**Soffietti et al., 2002]. Baseline symptoms of fatigue, nausea, appetite loss and also depression, were significantly related to shorter overall survival in patients with brain metastases [Wong et al., 2016]. The most adequate therapy for patients with brain metastases is based on several prognostic scores [e.g., Recursive Partitioning Analysis (RPA), Score Index For Radiosurgery (SIR), Basic Score for Brain Metastases (BSBM)], which could be a useful tool for treatment management [Venur et al., 2015]. RPA classification is a widely used

and reliable prognostic score for brain metastases patients. The main prognostic factors for survival are KPS, control of primary tumor (3 months without active chemotherapy means that the primary tumor is controlled), age, and the status of extracranial disease. Based on these factors, three classes were separated using RPA classification. Class I includes patients with best survival (KPS>70, controlled primary tumor, age<65 years, only brain metastases; had a median 7.1 months survival), while class III (with a,b,c subgroups) includes patients with the worst survival (KPS<70; median 2.3 months). The rest of the patients were grouped Class II [Venur et al., 2015].

I.5. Neuroimaging in brain tumors

Brain tumors are diagnosed typically when they cause symptoms, when patients may undergo a brain CT scanning in the acute setting; however, conventional MR imaging with contrast administration is the standard clinical method for initial diagnosis of brain tumors and plays an important role for differentiation, presurgical evaluation, treatment planning, and post-treatment follow-up. In addition, advanced MRI techniques, such as diffusion-weighted imaging (DWI), perfusion-weighted imaging (PWI) and MR spectroscopy (MRS) add important information for tumor diagnosis and management and are also promising techniques in the identification of potential molecular characteristics of brain tumors [Castellano & Falini, 2016]. Molecular imaging with positron emission tomography (PET) also plays an increasing role in selected subgroups of patients with pre- and post-treatment brain tumors, both in adults and in pediatric brain tumors [Gulyás & Halldin, 2012; Juhász & Bosnyák, 2016].

I.5.1. Conventional MRI in the initial diagnosis of primary brain tumors

Low-grade gliomas are typically seen as a non-enhancing lesion on MRI, while grade III anaplastic glioma and GBM often present as contrast-enhancing lesions on MRI. The typical radiographic features of GBM on post-contrast T1 images include thick irregular ring of heterogeneous enhancement surrounding a central necrosis, often with a larger area of peritumoral hyperintensity on fluid-attenuated inversion recovery (FLAIR) and T2-weighted sequences, representing the region of tumor infiltration and vasogenic edema [Osborn et al., 2010; Zinn & Colen, 2013]. Although conventional MRI (e.g. FLAIR) is able to detect even very small brain lesions, as we have proven in migraine [Erdélyi-Bótor et al., 2017], due to its relatively good spatial resolution, it has a limited ability to differentiate low-grade from high-grade (infiltrative) tumors and also recurrent/progressing brain tumors from radiation injury. In fact, in infiltrative tumors, such as glioblastoma, neoplastic cells extend beyond the tumor area detected by conventional MRI into areas of normal-appearing white matter [Osborn et al., 2010].

Meningiomas can be diagnosed by conventional MRI, such as pre- and post-contrast T1-weighted, T2-weighted and FLAIR images; however, MRI has a limited ability to differentiate low-grade from high-grade meningiomas or tumor tissue from non-specific tissue changes, such as radiation necrosis [Cha, 2009]. Meningiomas usually present as a solitary, enhancing lesion attached to the dura mater. Typical appearance of grade I meningiomas is isointense on pre- and show enhancement on post-contrast T1-weighted MRI, while iso- or hyperintense on FLAIR images. Thickening of the dura at the perimeter of the tumor (called dura-tail) can be seen on post-contrast images [Takeguchi

et al., 2004]. Grade II meningiomas cannot be distinguished clearly from grade I tumors by MRI, while anaplastic meningiomas (grade III) are often irregularly shaped [Zhang et al., 2008], and also invasion of the cortex and diffuse growth might be seen [Lin et al., 2014]. CT is useful to detect the calcification within the tumor, as well as hyperostosis of adjacent bones and intraosseous tumor growth, especially in skull-base meningiomas.

I.5.2. Conventional MRI in recurrent gliomas: RANO criteria

In current clinical practice, conventional MRI, such as T2-weighted, FLAIR, and, particularly, pre- and post-contrast T1-weighted MRI are the gold standard diagnostic tools not only in the initial diagnosis but also in post-treatment evaluation of brain tumors. In post-treatment evaluation, pseudo-progression and also pseudo-response (for example, after treatment with antiangiogenic agents) are a common challenge. Progressive disease may be diagnosed by Response Assessment in Neuro-Oncology (RANO) criteria in high-grade gliomas [Eisele et al., 2016]. Main criteria of tumor progression include a 25% increase in the sum of perpendicular diameters of the enhancing mass detected in 4-week intervals; or a new lesion or substantially worsened T2/FLAIR signal, or clinical decline (**Table 4)**.

Table 4. RANO criteria in high-grade gliomas

RANO - High-grade glioma	
Imaging modality	MRI or CT
Imaging intervals	At least 4 weeks
Measurable Disease	Up to 5 contrast-enhancing lesions
	Characterized by ≥10 mm longest and ≥5 mm perpendicular diameter
Response Assessment	
Complete response (CR)	Disappearance of all enhancing disease for ≥4 weeks
	No new lesions
	Stable or improved T2/FLAIR
	No more than physiological steroids
	Clinically stable or improved
Partial response (PR)	≥50% decrease in the sum of perpendicular diameters of enh. disease for ≥4 weeks
	No new lesion
	Stable or improved T2/FLAIR
	Stable or decreased steroid dose
	Clinically stable or improved
Stable Disease	Changes do not qualify for CR, PR or progressive disease
	No new lesion
	Stable or improved T2/FLAIR
	Stable or decreased steroid dose
	Clinically stable or improved
Progressive Disease	≥25% increase in the sum of perpendicular diameters of enhancing disease for ≥4 weeks
	Or new lesion
	Or substantially worsened T2/FLAIR
	Or substantial clinical decline

There are also some criteria to distinguish complete therapeutic response from pseudo-response. Pseudo-response is defined as a decrease of contrast enhancement without a true anti-tumor effect, which can be seen in 20–60 % of patients who receive VEGF-targeted therapy (i.e., bevacizumab) for high-grade glioma and is attributed to normalization of abnormally permeable blood vessels within the tumor [Eisele et al., 2016].

Recently, clinical trials with immunotherapy have been initiated in brain tumors. RANO criteria may not correctly capture treatment responses during such treatment. Therefore, immunotherapy-RANO [iRANO] criteria have been developed to establish appropriate imaging criteria optimized to follow the immune therapy response [Okada et al., 2015].

The iRANO recommends that if there is radiographic progression without clinical progression, immunotherapy should be continued and MRI repeated after 3 months. Progressive disease should be established only if the follow-up MRI shows further progression. Otherwise, if the repeat MRI is stable or shows improvement, the immunotherapy should be continued [Eisele et al., 2016]. In addition, iRANO recommends the minimal use of steroids because of their potentially negative effects on the efficiency of immunotherapies [Okada et al., 2015].

Despite its widespread clinical use, conventional MRI is not a reliable technique in differentiation of real tumor recurrence from radiation injury or pseudo-progression, which might be associated with temozolomide chemotherapy [Macdonald et al., 1990; Eisele et al., 2016]. Therefore, advanced MRI techniques play an increasingly important role in the post-treatment evaluation of brain tumors.

I.5.3. Advanced MRI (MR Spectroscopy, Perfusion, and Diffusion Imaging)

In the last decade, advanced MRI techniques have been under intense investigations as promising diagnostic tools in both newly diagnosed and previously treated brain tumors [Barajas et al., 2010; Dhermain et al., 2010]. DWI, PWI and MRS can provide detailed physiologic information about several tumor characteristics, such as vascularisation, microperfusion, and cellularity [Al-Okaili et al., 2006; Zinn & Colen, 2013], and they

have shown a promise in the post-treatment evaluation of malignant gliomas [Dhermain et al., 2010]. DWI can estimate tumor density and can be useful to differentiate non-enhancing tumor area from peritumoral edema in white matter [Bruzzone et al., 2012]. PWI can predict the tumor grade based on the assessment of angiogenesis and blood brain barrier permeability [Law et al., 2004; Bruzzone et al., 2012;]; also it might be an important diagnostic tool during antiangiogenic therapy [Law, 2009]. In addition, MR perfusion can play a significant role in neuro-oncology as a noninvasive diagnostic tool for prognosis and response to therapy [Law, 2009].

MR spectroscopy measures tumor-related changes of various metabolites, such as choline, creatine, N-acetylaspartate (NAA) or lactate, which can be associated with the tumor grade [Al-Okaili et al., 2006]. Changes in these metabolites can also estimate the proliferation rate of tumor cells (based on choline/NAA) and presence of necrosis (lipids or lactate peak) [Young, 2007; Dhermain et al., 2010].

Imaging correlates of tumoral genomic changes (radiogenomics) is an intensely investigated topic of tumor biology to establish correlations between MRI parameters and genetic expression patterns [ElBanan et al., 2015]. In the near future, these approaches can play an important role in pretreatment evaluation, treatment planning, and also in the post-treatment follow-up of patients with malignant glioma.

I.5.4. PET imaging

In neuro-oncology, molecular imaging with PET can play an important additional role in diagnosis and management. PET can detect and characterize different types of tumors,

including brain tumors, based on their metabolic properties, such as altered glucose, nucleoside and amino acid metabolism.

I.5.4.1. FDG-PET: 2-deoxy-2[^{18}F]fluoro-D-glucose (FDG) PET has evolved over the past three decades into a key clinical PET modality in detecting both intra- and extracranial tumors. Increased FDG uptake is common in highly proliferating cells because the tumor cells have increased expression of glucose transporters and hexokinase, the enzyme that converts glucose (and FDG) to a phosphorylated product [Smith, 2001]. FDG uptake is proportional to glucose uptake although not quantitatively equal to glucose metabolism. In neuro-oncology, the primary goal of FDG-PET is differentiation of malignant from benign lesions and distinguishing recurrent tumors from radiation injury. The main advantages of FDG include its relatively long half-life (110 minutes due to F-18) and its streamlined radio-synthesis. However, inflammatory lesions also accumulate FDG [van Waarde & Elsinga, 2008], and the high baseline of glucose metabolism in the cerebral gray matter can diminish the contrast between malignant tumors and normal brain tissue. Also, FDG uptake is low in most low-grade gliomas, and FDG-PET also shows limited specificity in identifying recurrent tumors. Therefore, clinical applications of other types of PET tracers, such as radiolabeled amino acids, have been tested during the last decade.

I.5.4.2. Amino acid PET: Most tumors have higher amino acid uptake and metabolism than normal cells. This difference is the basis of the high sensitivity of amino acid PET in cancer imaging [Huang & McConathy, 2013]. The most widely tested amino acid PET tracers in brain tumor imaging include L-[methyl-^{11}C]methionine (MET), ^{18}F-fluoroethyl-tyrosine (FET), and ^{18}F-fluoro-L-dihydroxy-phenylalanine (FDOPA); the group at Wayne

State University has also introduced the human use of ^{11}C-alpha-methyl-L-tryptophan (AMT) in cancer imaging (Juhasz et al., 2006 [brain tumors]; 2009 [lung cancer]; 2012 [breast cancer]; see also review in Juhasz et al., 2014). MET is the most widely studied PET tracer in brain tumor imaging, although it is labeled with the short half-life (20 min) carbon-11 positron-emitting isotope [Glaudemans et al., 2013; Galldiks et al., 2011]. Similar to FDG, FET is labeled with F-18, which has a 110 min half-life more suitable for routine clinical applications [Heiss et al., 1999; Wester et al., 1999]. Both MET- and FET-PET can detect and differentiate newly diagnosed and recurrent gliomas, and provide useful information in initial treatment planning and response monitoring [Dunet et al., 2012; Gulyas & Halldin, 2012; Nihashi et al., 2013; Glaudemans et al., 2013; Gotz & Grosu, 2013]. FDOPA, originally developed to measure dopamine synthesis [Eidelberg et al., 1993; Matsubara et al., 2011], is used in a few centers for brain tumor imaging; it has with similar kinetic characteristics to FET [Becherer et al., 2003; Schiepers et al., 2007; Chen et al., 2006; Fueger et al., 2010].

The L-type amino acid transporters (LATs) play a central role in amino acid transport from the blood to brain and tumor tissue. LAT1, LAT2, LAT3 and LAT4 all transport neutral amino acids, but LAT1 is most widely expressed in primary human cancers and cancer cell lines and plays a significant role in survival and tumor growth [Imai et al., 2010; Alkonyi et al., 2012; Zitron et al., 2013]. The metabolic fate of various amino acid PET tracers after initial transport is variable: they can be trapped without any metabolic changes (such as the case of FET), may get incorporated into proteins (such as MET) and/or metabolized via different metabolic pathways (FDOPA or AMT).

1.5.4.3. AMT-PET: ^{11}C-alpha-methyl-L-tryptophan (AMT) was developed originally to estimate brain serotonin synthesis rates [Diksic et al., 1990; 1991]. Increased cortical AMT uptake can also to identify epileptogenic foci in patients with drug resistant epilepsy, especially in patients with various developmental abnormalities and lesions [Chugani et al., 1998; Juhasz et al., 2003]. In initial studies of AMT-PET in brain tumors, high tryptophan uptake was detected in a variety of low-grade and high-grade brain tumors [Juhasz et al., 2006, Juhász et al., 2011; Alkonyi et al., 2012]. In addition to measuring static tumoral AMT uptake, tracer kinetic analysis [Patlak et al., 1983] was found to be useful in differentiation low-grade tumor types [Juhasz et al., 2011], estimate tumor proliferative activity [Juhasz et al., 2012], and differentiate recurrent tumor from radiation necrosis [Alkonyi et al., 2012, Kamson et al., 2013, Bosnyák et al., 2015]. We have also demonstrated that combination of AMT-PET with advanced MRI, such as diffusion tensor imaging, can facilitate non-invasive estimation of tumor cellularity [Jeong et al., 2015].

Tryptophan and AMT are mostly transported into brain tumor tissue via LAT1 [Alkonyi et al., 2012; Haining et al., 2012; Juhasz et al., 2012]. However, AMT, unlike tryptophan, is not incorporated into proteins, because of the added methyl group in the alpha position [Diksic et al., 1990; Nagahiro et al., 1990]. Tryptophan can be metabolized via the immunomodulatory kynurenine pathway (KP) (**Figure 1**), which plays a key role in tumoral immune tolerance [Uyttenhove et al., 2003; Munn & Mellor, 2007]. AMT can also undergo enzymatic conversion via the initial and rate-limiting KP enzyme indoelamine 2,3-dioxygenase (IDO), and trapped as a labeled metabolite [Chugani et al., 2000; Batista et al., 2009].

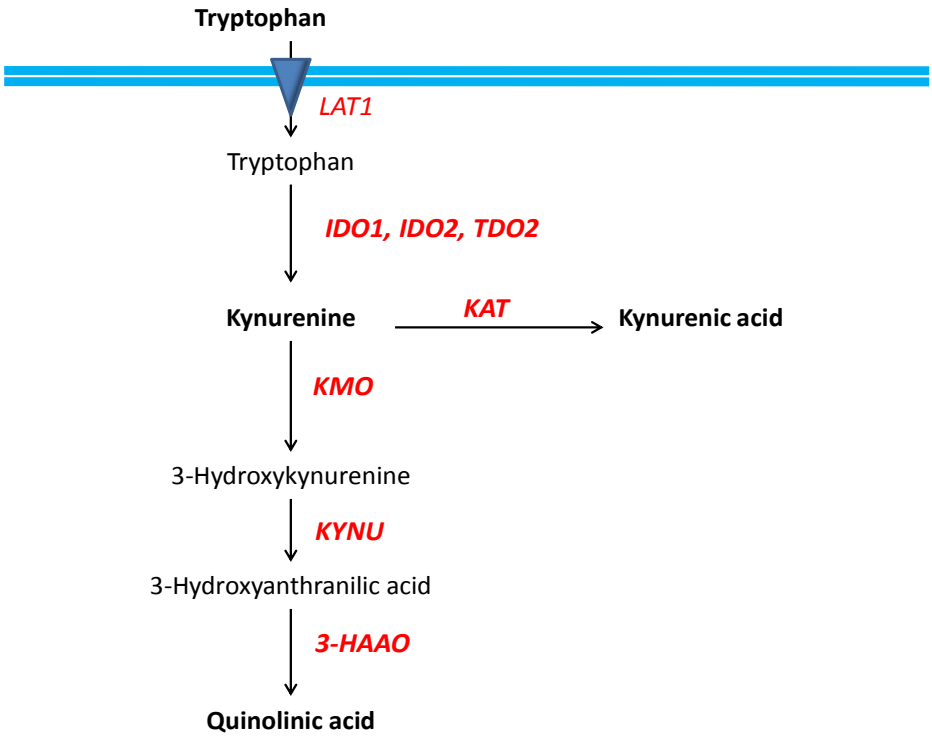

Figure 1. **Key transporter, metabolites and enzymes of the kynurenine pathway.** LAT1: L-type amino acid transporter; IDO: Indoleamine 2,3-dioxygenase; TDO: Tryptophan 2,3-dioxygenase; KAT: Kynurenine aminotransferase; KMO: Kynurenine 3-monooxygenase; KYNU: Kynureninase; 3-HAAO: 3-Hydroxyanthranilic acid oxygenase. Tumoral conversion of tryptophan to kynurenine can be mediated by 3 enzymes: IDO1, IDO2 and TDO2.

High expression and activity of IDO is known to induce an immunosuppressive tumoral microenvironment by creating immunosuppressive metabolites such as L-kynurenine [Munn and Mellor, 2007]. High kynurenine concentration can lead to suppression of natural killer cells and generation of regulatory T cells, thus promoting the escape of tumor cells from the host immune response. IDO is overexpressed in various tumors, including malignant gliomas [Uyttenhove et al., 2003; Batista et al., 2009; Pilotte et al., 2012; Mitsuka et al., 2013]. High IDO protein expression, detected by immunostaining, was found in primary brain tumors showing high AMT trapping [Batista, 2009; Alkonyi et al., 2012]. Based on these studies, high AMT uptake and accumulation may be an

imaging marker of high LAT1 and IDO activity, respectively. Conversion of tryptophan to kynurenine can be mediated by three distinct enzymes: IDO1, IDO2 as well as tryptophan 2,3-dioxygenase 2 (TDO2), all of which could be targeted by inhibitors to alleviate tumoral immune resistance to enhance the effects of chemo- or immunotherapy [Opitz et al., 2011; Austin & Rendina, 2014].

II. OBJECTIVES

The overall aim of our studies was to explore the potential clinical use of AMT-PET in both newly diagnosed and recurrent brain tumors. We focused on applications where amino acid PET has not been used or validated before. The objectives of four published studies are summarized below.

In Study 1, we had two main goals: i. To evaluate if prognostic molecular markers in primary (IDH1 wild-type) glioblastomas are associated with a specific pattern of amino acid uptake or metabolism on PET imaging and/or MRI variables; ii. To determine if pre-treatment tryptophan uptake measured by PET has a prognostic value for overall survival in the same group.

In Study 2, we evaluated the clinical value of high AMT uptake in brain regions outside the contrast-enhancing tissue in post-treatment glioblastomas. Specifically, we tested if non-enhancing brain regions showing increased AMT uptake predict the spatio-temporal pattern of tumor progression during imaging follow-up.

In Study 3, we explored the potential role of abnormal tryptophan metabolism in brain tumor-associated depression. The overall goal was to determine if abnormal brain tryptophan metabolism in non-tumoral brain regions, measured by PET, could be an imaging biomarker for brain tumor-associated depression.

In Study 4, we evaluated mechanisms and potential clinical significance of abnormal tryptophan uptake and metabolism in WHO grade I–III meningiomas using AMT-PET with detailed tracer kinetic analysis. We also assessed if AMT kinetic characteristisc are related to meningioma expression of key enzymes of the kynurenine pathway.

In the next sections, we first describe the common imaging protocol and analysis approaches used in all studies, and then provide details on subjects and results for each individual study.

III. METHODS

III.1. Magnetic Resonance Imaging

Diagnostic MRI scans with routine pre/post-gadolinium T1 (T1-Gad), T2-weighted, and FLAIR axial images acquired closest in time (typically within 2 weeks) to the AMT-PET were used in our studies. MRI was performed on one of three 3T scanners located at the Detroit Medical Center / Karmanos Cancer Institute campus, using similar parameters: (i) Siemens MAGNETOM Trio TIM (Siemens Medical Solutions, Malvern, Pennsylvania); (ii) GE Signa HDxt (GE Medical Systems, Milwaukee, Wisconsin); or (iii) Philips Achieva TX (Philips Medical Systems Inc., Da Best, the Netherlands).

In Study 2 (post-treatment tumor progression), we also reviewed T1-Gad MRI scans acquired after AMT-PET during clinical follow-up, and further analyzed the first MRI that showed a clear progression (enlargement) of the contrast-enhancing lesion, in those patients where such a progression occurred within the 2-year follow-up period.

III.2. AMT-PET acquisition

The AMT-PET studies were performed using a GE Discovery STE PET/CT scanner (GE Medical Systems, Milwaukee, WI) or a Siemens EXACT/HR whole-body positron emission tomograph (Siemens Medical Systems, Knoxville, TN) located at the PET Center, Children's Hospital of Michigan in Detroit. Both scanners have a 15-cm field of view and generate 47 image planes with a slice thickness of 3 mm. The reconstructed image in-plane resolution was 7.5±0.4 mm at full-width half-maximum (FWHM) and 7.0±0.5 mm at FWHM in the axial direction (reconstruction parameters: Hanning filter with 1.26 cycles/cm cutoff frequency) for the Siemens scanner. The GE scanner has a

similar resolution, with FWHM of 7.5 mm (isotropic), and images from this scanner were reconstructed with an iterative reconstruction (2 iterations, 16 subsets, 8-mm axial smoothing). The AMT tracer was synthesized using a high-yield procedure as previously outlined [Chakraborty et al., 1996]. For AMT-PET scanning, patients fasted for 6 hours to ensure low blood tryptophan levels. A slow bolus of AMT (3.7 MBq/kg=1mCi/kg) was injected intravenously over 2 minutes. For collection of timed blood samples, a second venous line was established. In the initial 20 minutes of the scan following tracer injection, a dynamic PET scan of the heart was performed to obtain the blood input function from the left cardiac ventricle noninvasively. The blood input function was continued beyond these initial 20 minutes by using venous blood samples (0.5 mL/sample, collected at 20, 30, 40, 50, and 60 min after AMT injection). At 25 minutes after tracer injection, a dynamic emission scan of the brain (7×5 min) was obtained. Measured attenuation correction, scatter, and decay correction were applied to all PET images.

III.3. AMT-PET Image Processing

For visualization of AMT uptake in the brain, averaged activity images 30–55 minutes post injection were created and converted to an AMT standardized uptake value (SUV) image. For quantification of AMT transport and accumulation, a Patlak graphical analysis was performed using the dynamic brain PET images and blood input function [Patlak et al., 1983; Juhasz, et al., 2006]. This approach provides two kinetic parameters: The y intercept of the Patlak plot (see an example below in **Figure 9**, below in the Results section) yields the tracer's apparent volume of distribution (VD'), which is indicative of the net transport of tryptophan into the tissue of interest (tumor or cortex). The slope of the Patlak plot reflects the unidirectional uptake of tracer into the tissue (K-complex) and

correlates with tryptophan metabolism via the serotonin synthesis pathway in cortex [Chugani & Muzik, 2000]. In brain tumors with no evidence of serotonin synthesis, the most likely mechanism of an increase in AMT K-complex is tumoral accumulation in the form of kynurenine metabolites if key enzymes such as IDO (or TDO) are present and active [Chugani & Muzik, 2000]. In addition, the ratio between K and VD′ yields parameter k_3', an estimate of the k_3 parameter that characterizes the irreversible trapping of AMT, presumably due to enzymatic conversion to α-methyl-L-kynurenine.

III.4. Multimodal Image Analysis

For multimodal image analysis, the 3D Slicer 3.6.3 software suite was used (http://www.slicer.org; Brigham and Women's Hospital, Inc.) [Kikinis & Pieper, 2011] as described previously [Kamson et al., 2014]. First, a transformation matrix was created by co-registration of the summed AMT-PET images to the T1-Gad volumetric image volumes (magnetization-prepared rapid gradient-echo [MPRAGE] protocol on Siemens or MPRAGE-equivalent sequence on GE and Philips scanners) as well as FLAIR images using the Fast Rigid Registration module [Mattes et al., 2003]. This transformation matrix was then applied to the summed AMT-PET image and to the dynamic AMT-PET images loaded via the 4D image module of 3D Slicer. Regions of interest (ROIs) were drawn on the tumor mass in tumor regions with MPRAGE contrast enhancement and/or T2/FLAIR signal changes on MRI, and the ROIs were then applied on the co-registered AMT SUV as well dynamic PET images, where applicable. As a reference (background) region, at least 3 ROIs were drawn on the homotopic cortex (normal on MRI) contralateral to the tumor, and the values from these ROIs were averaged. The 3D Slicer was also used for threshold-based volume of interest (VOI) analysis [Kikinis & Pieper, 2011]. The volume

of increased AMT SUV in and around the contrast-enhancing area was determined based on a cutoff threshold (>65 % increase as compared to contralateral cortical AMT SUV) that provided excellent accuracy to differentiate progressing high-grade gliomas associated with short survival versus those with stable course and longer survival in our recent study [Kamson et al., 2014]. Voxels surviving this 65% cutoff threshold were summed and their volume (i.e., PET+ volume) was expressed in cm^3.

III.5. Tumor histopathology, glioma molecular markers and enzymes of the kynurenine pathway

Routine histopathology of all tumor specimens were performed at the Pathology Department of Wayne State University and reviewed by a board certificate pathologist who determined tumor type and grade. Ki-67 nuclear labeling (expressed in %) was used to determine the tumor proliferation index. Analysis of glioma molecular markers and key enzymes of the kynurenine pathway (KP) were performed at the Neuro-Oncology Research Laboratory, Department of Neurosurgery, Wayne State University. In Study 1, glioma markers including IDH1 mutation, EGFR amplification and MGMT promoter methylation status have been determined [Bosnyák et al., 2017]. In Study 4, expression of 5 key enzymes of the KP, such as IDO 1/2, TDO2, KYNU and KMO were assessed by immunohistochemistry in all meningioma samples [Bosnyák et al., 2015].

IV. SUBJECTS, STUDY DESIGN AND RESULTS OF THE INDIVIDUAL STUDIES

Our multimodal imaging studies included groups of adult patients with a variety of pre- and post-treatment brain tumors. A summary of the patient populations in the four studies is provided in **Table 5**. All studies were approved by the Institutional Review Board of Wayne State University and written informed consent was obtained from all participants. In all studies, the statistical analysis was performed using IBM SPSS Statistics for Windows, Version 19.0 (IBM Corp., Armonk, NY), 21.0., or 23.0. A p value of <0.05 was considered significant.

Table 5. Summary of tumor types in the four studies

Gr.: Grade; GBM: Glioblastoma

	Meningioma		**Low-grade (WHO Gr. II) glioma**		**WHO Gr. III glioma**	**GBM (WHO Gr. IV)**		**Metastasis**	**Total No.**
Treatment	pre	post	pre	post	post	pre	post	pre	
STUDY I.						21			**21**
STUDY II.							12		**12**
STUDY III.	9	1	2	1	1	3	1	3	**21**
STUDY IV.	16	0	16	0					**32**
Total No.	**25**	**1**	**18**	**1**	**1**	**24**	**13**	**3**	**86**

IV.1. *Study 1 – AMT-PET imaging of prognostic glioblastoma markers and survival*

(Bosnyák et al. Clin Nucl Med, 2017)

IV.1.1. Patient population

Twenty-one patients (14 males, mean age: 62 years) with a brain mass suspicious for glioblastoma underwent presurgical MRI and AMT-PET scanning followed by surgical resection and standard chemoradiation. In all patients, IDH1 wild-type glioblastoma was confirmed by histopathology. Thirteen patients had gross total tumor resection, while 8 had subtotal resection at initial surgery. Five patients underwent a second resection after tumor recurrence, and two patients received additional chemotherapy (bevacizumab and bevacizumab with irinotecan in one case each). The median survival time was 14.8 months, and 13 of the 21 patients (62%) had >1-year survival.

IV.1.2. Study design and statistical analysis

Tumor volumes on T2 and T1-Gad MRI were defined as described previously [Kamson et al., 2013]. Contrast-enhancing volumes were created by segmentation of post-contrast abnormalities semi-automatically, while T2 images were segmented manually to avoid erroneous inclusion of cerebrospinal fluid in the volume of interest. MRI characteristics (T2 and T1-Gad volume), tumoral AMT uptake variables (tumoral SUV, VD' and K, their tumor/cortex ratios), PET-based metabolic tumor-volume, and MRI/PET volume ratios were correlated with prognostic molecular markers (EGFR amplification and MGMT methylation status) and overall survival.

Group comparisons were performed using the Mann-Whitney U-test. Univariate correlations were performed using the Spearman’s rank correlation. After identifying the

PET variable(s) with a significant correlation with overall survival, a receiver-operating characteristic (ROC) analysis was performed to identify the optimal threshold for differentiating patients who were alive at 1-year follow-up from those who had died. Using this cutoff threshold, a Cox-regression analysis was done to obtain a hazard ratio (HR) for survival in patients having above- vs. below-threshold values.

IV.1.3. Results

IV.1.3.1 Relation of AMT-PET variables to glioma molecular markers. Mean Ki-67 labeling index was 30% (range: 10-70%), MGMT promoter methylation was present in 7/19 (37%; not available in 2 cases), while EGFR amplification was detected in 6/20 tumors (30%; not available in 1 case). EGFR amplification was associated with lower T1-Gad volume (P=.04), lower T1-Gad/T2 volume (P=.04) and T1-Gad/PET volume ratios (P=.02). Tumors with MGMT promoter methylation showed lower metabolic volume (P=.045) and lower tumor/cortex AMT K ratios than those with unmethylated MGMT promoter (P=.009).

IV.1.3.2. Prognostic value of AMT-PET for survival. Overall survival showed a significant positive correlation with tumor/cortex SUV-ratios (r=0.49; *P*=.023), indicating longer survival in those with higher pre-treatment tumoral tryptophan uptake (**Figure 2.**).

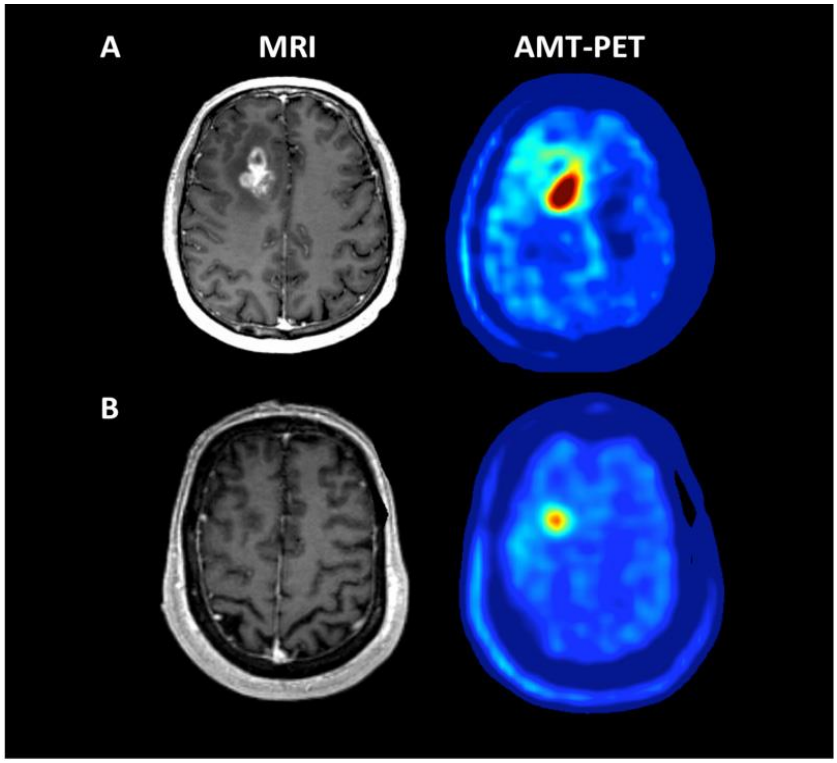

Figure 2. Representative examples of MRI (T1-Gad) and AMT-PET in a patient with high (**A**) vs. low (**B**) AMT uptake associated with different survival. (**A**) A 54 year-old male with a right frontal glioblastoma, measured with a 2.59 tumor/cortex AMT SUV-ratio, above the ROC-defined threshold of 1.94. He survived for more than 2 years after the PET scan. (**B**) A 68 year-old male with a right frontal glioblastoma showing a below-threshold tumor/cortex AMT SUV-ratio (1.56). He survived for only 7 months.

The ROC analysis showed high area under the curve (AUC) for AMT SUV-ratios (0.94; *P*=.001). Using the optimal 1.94 tumor/cortex SUV-ratio as the cutoff threshold, 1-year survival was correctly predicted with 100% sensitivity and 88% specificity. Cox-regression analysis showed that AMT SUV-ratios above 1.94 were prognostic for long survival (HR: 30.2 [95% CI: 3.5-259]; *P*=.002) (**Figure 3.**). Estimated mean overall survival was 26 months in patients with high (above-threshold) vs. 8 months in those with low (below-threshold) tumor/cortex AMT uptake ratios.

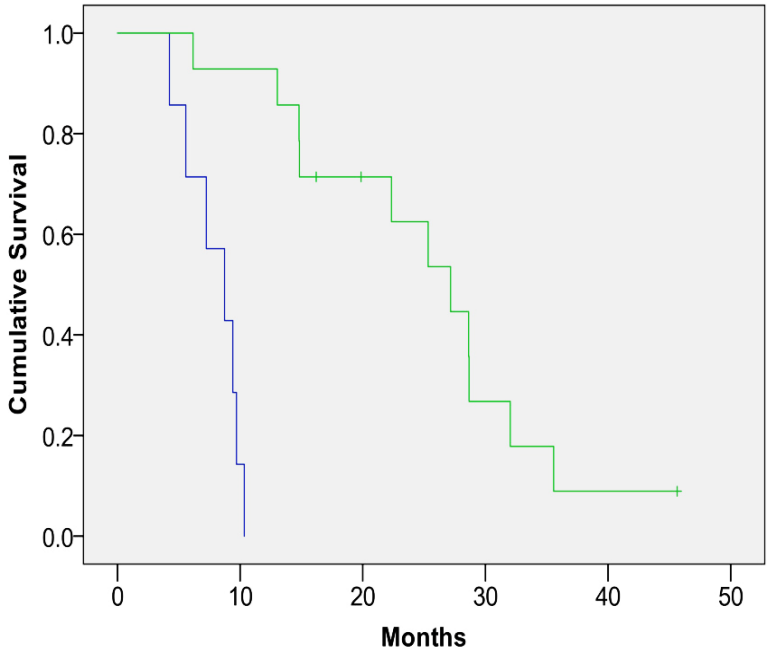

Figure 3. Kaplan-Meijer survival curves in patients with high (green) vs. low (blue) AMT uptake ratios (based on the cutoff threshold of 1.94 tumor/cortex SUV ratio, determined by an ROC analysis based on 1-year survival). Patients with above-threshold ratios had a substantially longer cumulative survival (HR: 30.2 [95% CI: 3.5-259]; P=.002).

IV.2. ***Study 2 - AMT-PET to predict progression of post-treatment glioblastoma***

(Bosnyák et al., J Neurooncol, 2016)

IV.2.1. Patient population

We investigated 12 patients (6 males, mean age: 61 years) with glioblastoma verified by histopathology, who underwent previous surgical resection followed by chemoradiation (Stupp regimen). All patients had a post-treatment AMT-PET scanning following an MRI that showed possible tumor progression (contrast-enhancing area) verified by a board-certified neuro-radiologist. After the AMT-PET scan, all patients were followed for up to 2 years with serial MRI scans at 1- to 2-month intervals until clear progression of the contrast-enhancing lesions was noted.

IV.2.2. Study design and analysis

IV.2.2.1. Image analysis: The volume of increased AMT SUV in and around the contrast-enhancing area was determined based on a cutoff threshold (>65% increase as compared to contralateral cortical AMT SUV) which can differentiate accurately high grade gliomas with short survival from those with longer survival [Kamson et al., 2014]. Voxels surviving this cutoff threshold were summed and their volume (i.e., PET+ volume) was expressed in cm^3. In addition, the area of contrast enhancement was delineated on the T1-Gad images, and its volume (Gad+ volume) was also calculated [Kamson, et al., 2013]. Subsequently, we also calculated the volume of increased (above-threshold) AMT SUV located outside the contrast-enhancing volume (i.e., Gad–/PET+ volume). The mean (SUV_{mean}) and maximum (SUV_{max}) AMT SUV were also measured in this area. Furthermore, we measured the maximum distance (in mm) between the outer edge of the area with increased AMT uptake and the edge of the Gad+ volume. Subsequently, we repeated the volumetric analysis on the MRI scans showing radiographic evidence for clear T1-Gad progression (present in ten patients), after these MR images were also co-registered with both the AMT-PET and the initial MR images. On the same MRI scans, showing T1-Gad tumor progression, we measured the Gad+ volume extending beyond the boundaries of the increased AMT uptake measured at baseline.

IV.2.2.2. Statistical analysis: Wilcoxon signed rank test was utilized for the comparison of the PET+ volume extending beyond the Gad+ volume before versus after MRI progression. Time to MRI progression was compared between subgroups showing different patterns of progression using Mann–Whitney U test. Further, AMT-PET and T1-Gad volume parameters as well as SUV_{mean} and SUV_{max} measured in the Gad-/PET+ areas were correlated with the time to progression using Spearman's rank correlations.

IV.2.3. Results

In 10 patients with clear progression of the contrast-enhancing lesion (1-17 months after the PET scan), the non-enhancing PET+ volumes predicted the location of new enhancement, which extended beyond the PET+ brain tissue in six. In these six patients, the Gad+ region after progression not only invaded the PET+ brain tissue but extended considerably beyond it, with a widely varied volume (7.8–45 cm^3) (**Figure 4.**).

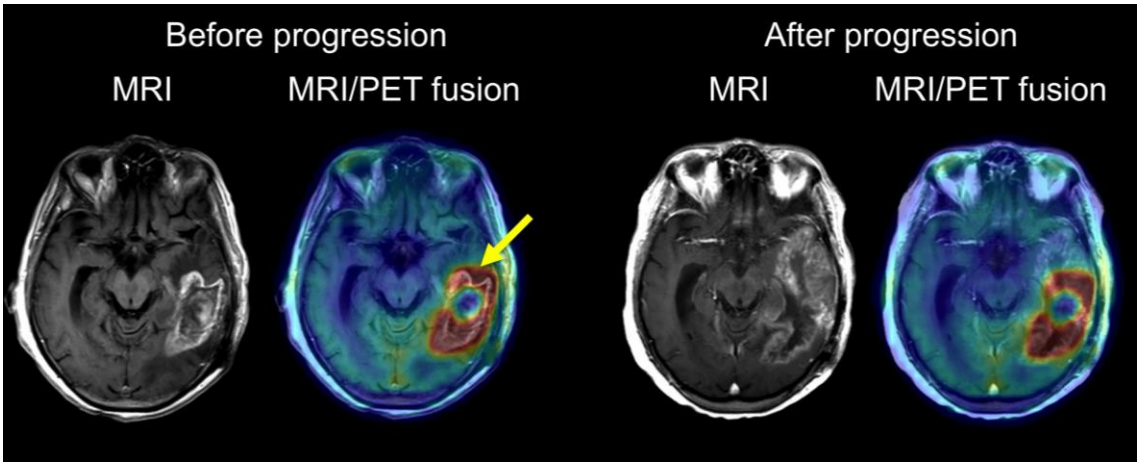

Figure 4. Glioblastoma progression with a large contrast-enhancing area and high AMT uptake in the left temporal region. The PET+ area extended anterior to the Gad+ lesion (arrow), with an SUV_{max} of 5.4. T1-Gad MRI 5 months later showed extension of the contrast enhancement into the anterior temporal lobe encompassing and extending beyond the baseline PET+ region.

In the other four patients with tumor progression, the Gad+ volume expansion mirrored the PET+ volume but with no or minimal extension beyond the PET+ area (**Figure 5A**). Two patients underwent second surgery and active glioblastoma was verified by histopathology. All patients showed clinical progression and deceased within 1-20 months. In two patients, with no PET+ area beyond the initial contrast enhancement, MRI remained stable during the 2-year follow-up (**Figure 5B**).

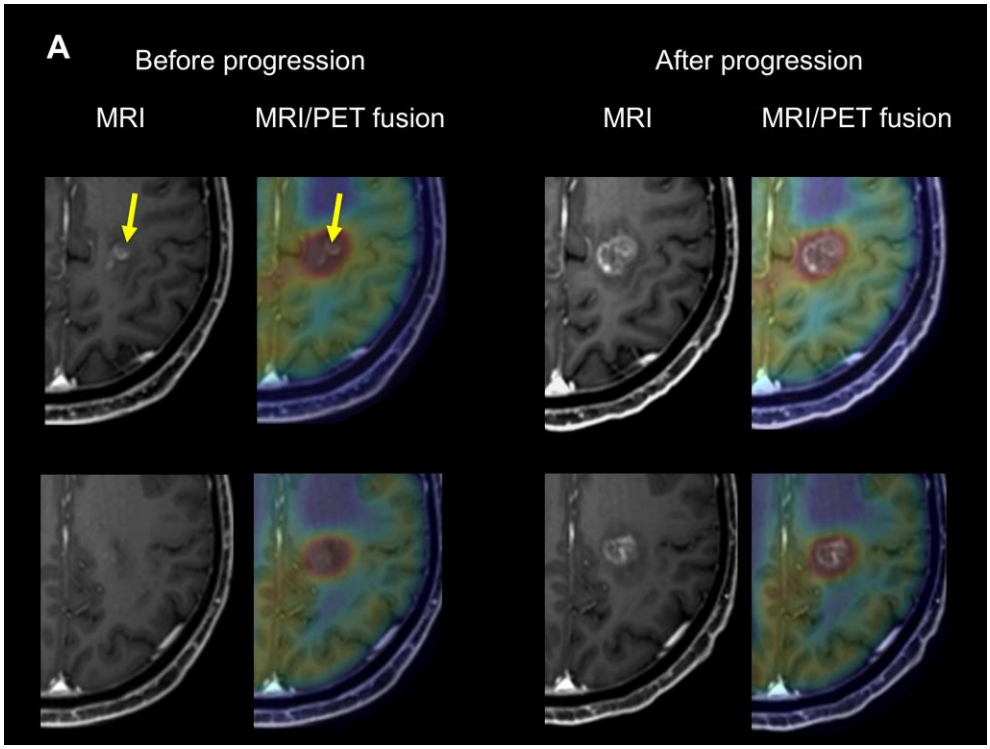

Figure 5A. T1-Gad MRI and co-registered MRI/AMT-PET fusion images of patient showing a left medial fronto-parietal contrast-enhancing lesion (arrows) suspicious for glioblastoma recurrence 4 months after initial treatment. High AMT uptake was seen in the same region (upper panel), extending superior (and also inferior and lateral) to the contrast-enhancing lesion (lower panel), with an SUV_{max} of 4.7. After MRI progression, 1 month later, the Gad+ mass grew into and filled the original PET+/Gad- area.

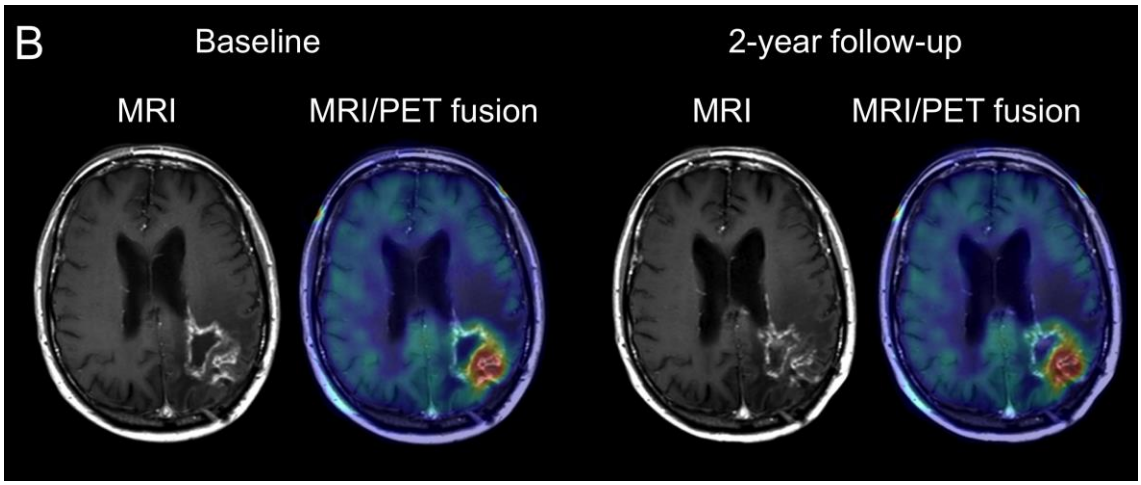

Figure 5B. T1-Gad MRI and MRI/AMT-PET fusion images of a left parieto-occipital tumor. The PET+ area was congruent with the bulk of the Gad+ lesion; no progression during the 2-year follow-up; SUV_{max} was below 4 (3.8).

There was a negative correlation between both AMT SUV_{mean} and SUV_{max} and time to progression (after PET) (SUV_{mean}: r = -0.77, p = 0.003; SUV_{max}: r = -0.69, p = 0.014), indicating a faster progression in those with higher AMT uptake in the non-enhancing brain. Patients with SUV_{max}>4 progressed within about 5 months, while patients with SUV_{max}<4 were progression-free on MRI scans at least 6 months.

IV.3. *Study 3 - Tryptophan metabolism in brain tumor-associated depression*

(Bosnyák et al., EJNMMI Research, 2015)

IV.3.1. Patient population

Study population included 21 patients (mean age: 57 years) with a variety of brain tumors. Histopathology verified 10 WHO grade I meningiomas, 8 WHO grade I-IV gliomas (including n=1 grade I, n=2 grade II, n=1 grade III and n=4 grade IV) and 3 patients with

brain metastases. Four out of 21 patients had previous resective surgery before with or without subsequent chemoradiation. Follow-up MRI showed tumor progression or recurrence in all 4 patients, and one patient had clinical progression as well. None of the 21 patients had a history of clinical depression and were not on any antidepressant medication at the time of AMT-PET. KPS in all patients was 70 or higher. Six of the 21 patients were on dexamethasone (which did not affect AMT kinetic values in a previous study [Juhász et al., 2012]), 10 patients had a history of seizure(s), and 12 were on antiepileptic medication at the time of the PET scan.

IV.3.2. Study design and analysis

IV.3.2.1. For the *assessment of depression*, the Beck Depression Inventory, 2nd Edition (BDI-II) was used [Beck et al., 1996]. The BDI-II is a self-reported measure that identifies the presence and severity of symptoms of depression. There are 21 items on the BDI-II each rated on a four-point Likert scale (0–3). The measure yields a total score, and the cutoffs for depression severity are as follows: 0–13 = no/minimal depression, 14–19 = mild depression, 20–28 = moderate depression, and 29–63 = severe depression. The psychometric properties of the scale have been well established, and the measure is widely used with both clinical and research samples including different cancer patient groups [Rooney et al., 2011; Mainio et al., 2005; Pelletier et al., 2002; Dozois et al., 1998; Storch et al., 2004].

IV.3.2.2. Statistical analysis: First, BDI-II depression scores were compared among three tumor types (gliomas, meningiomas, metastases) using the Kruskal-Wallis test. BDI-II depression scores were also correlated with tumor type, histologic grade (in primary brain

tumors), tumor size, and AMT-PET variables in the whole group as well as subgroups (patients with a primary brain tumor, patients with an intraaxial tumor [glioma or metastasis], and patients with a newly diagnosed tumor) using Spearman's rank correlations. AMT kinetic variables (K-complex or K and VD') were compared between depressed (BDI-II score >13) and non-depressed patients, as well as between moderately/severely depressed patients (BDI-II score ≥20) vs. the rest of the patients, using the Mann-Whitney U test.

IV.3.3. Results

The mean BDI-II score of the 21 patients was 12±10 (range: 2–33); clinical levels of depression were identified in seven patients (33 %). High BDI-II scores were most strongly associated with high thalamic AMT K values (**Figure 6**) both in the whole group (p= 0.004) and in the subgroup of 18 primary brain tumors (r = 0.68, p = 0.004).

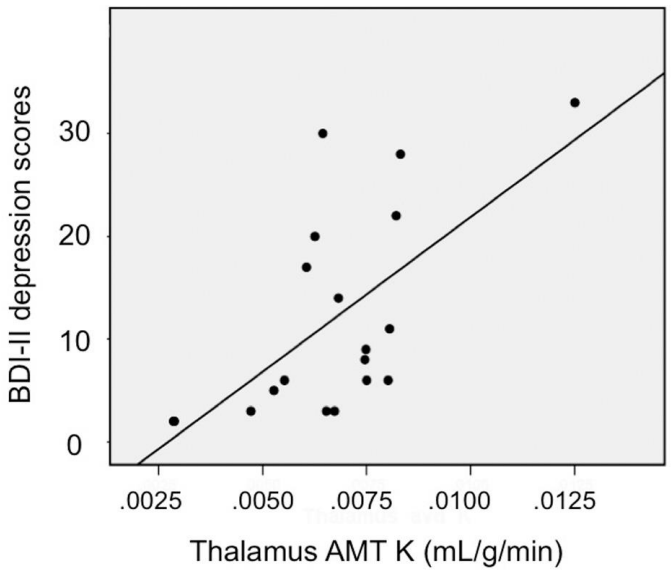

Figure 6. Positive correlation between thalamus AMT K values, measured by PET, and BDI-II depression scores (Spearman's rho = 0.63, p = 0.004).

Frontal and striatal VD' values were higher in the depressed subgroup than in non-depressed patients ($p < 0.05$) (**Figure 7**); the group difference was even more robust when moderately/severely depressed patients were compared to patients with no/mild depression (frontal: $p = 0.005$; striatal: $p < 0.001$). Tumor size, grade, and tumor type were not related to depression scores.

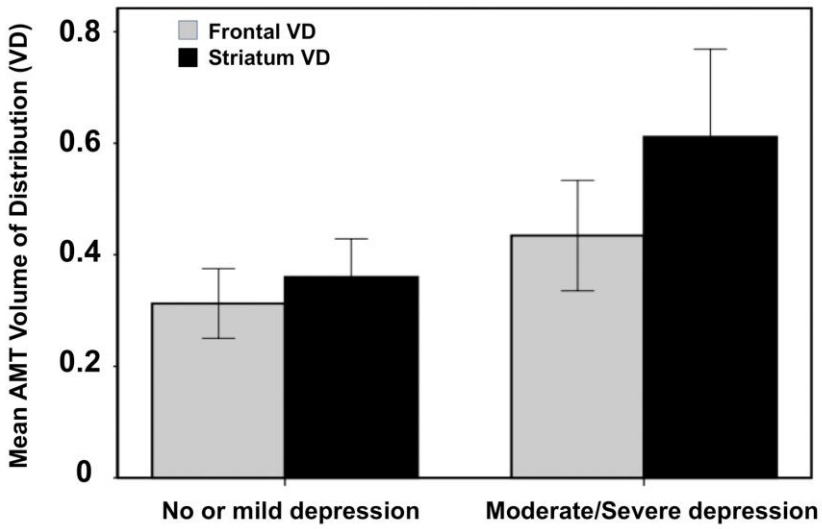

Figure 7. Comparison of AMT-PET variables in patients with no/mild depression vs. moderate/ severe depression. Frontal and striatal VD' values were significantly higher in patients with moderate/ severe depression (Frontal VD': 0.43 vs. 0.31, $p = 0.005$; striatal VD': 0.61 vs. 0.35; $p < 0.001$).

IV.4. *Study 4 - Tryptophan metabolism in meningiomas*

(Bosnyák et al., Neuro-Oncology, 2015)

IV.4.1. Patient population

In this study, we enrolled 47 patients (26 males) with meningioma (n=16, mean age: 56.9 years) and glioma (n=31, mean age: 42.9 years) who underwent presurgical MRI and AMT-PET scanning followed by surgical resection. Meningioma was confirmed in 16 patients (n=10 grade I; n=5 grade II and n=1 grade III) by histopathology, 21 patients had low-grade glioma (n=12 grade II oligodendroglioma, n=4 grade II mixed oligo-astrocytoma, n=5 grade II astrocytoma), while the remaining 10 patients had grade III glioma (n=5 astrocytoma, n=3 mixed oligo-astrocytoma, and n=2 oligodendroglioma).

IV.4.2. Study design and statistical analysis

AMT-PET parameters and tumor size (maximum area) were compared between the meningioma and glioma subgroups using unpaired *t* tests. The optimal cutoff threshold of the best AMT-PET parameter to differentiate meningiomas from gliomas (both low-grade and high-grade, separately) was established by ROC analysis, and the differentiating accuracy of the parameter was calculated. Further, AMT-PET variables in the meningioma group were correlated with patient age, tumor size, and histological grade as well as the Ki-67 labeling index (%), using Pearson's correlations. To test the accuracy of the best PET parameter (k_3') to differentiate low-grade and high-grade meningiomas, a ROC analysis was performed again. Confidence intervals for the AUC and accuracy using the optimum threshold from the ROC were calculated using bootstrapping with 10 000 bootstrap replicates. To determine the accuracy of the best AMT-PET parameter for

differentiating grade I versus grade II-III meningiomas, an optimal cutoff threshold was again established using ROC analysis, and the sensitivity and specificity of the parameter for differentiating these two meningioma grade groups were calculated. Immunostaining scores of the different KP enzymes were compared using a Wilcoxon signed-rank test. Enzyme expression scores between low-grade and high-grade meningiomas were compared using the Mann-Whitney U test. Finally, we correlated KP enzyme immunostaining scores with AMT-PET kinetic parameters using the Spearman's rank correlation.

IV.4.3. Results

This study described 3 novel findings. First, meningioma grade showed a significant positive correlation with AMT k_3'tumor/cortex ratio ($p = 0.003$), and this PET parameter distinguished grade I from grade II/III meningiomas with a 92% accuracy (**Figure 8.**).

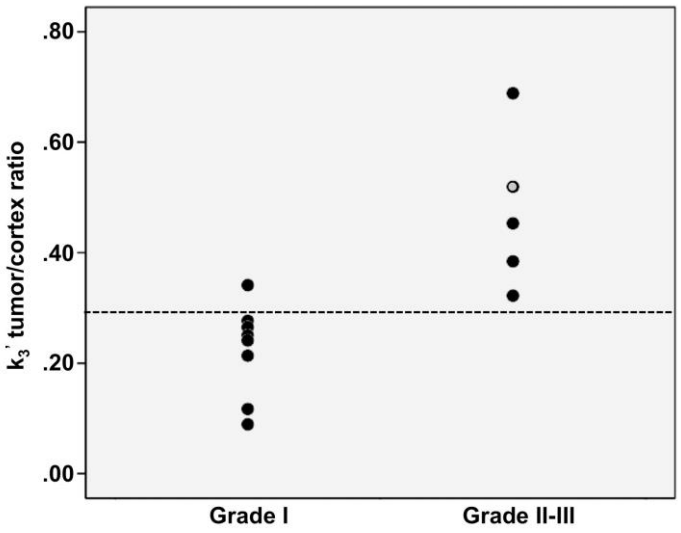

Figure 8. WHO grade I meningiomas showed lower tumor/cortex k_3'-ratios than grade II–III meningiomas. A k_3'-ratio threshold of 0.3 (based on the ROC analysis; the threshold level is indicated by a dotted line) distinguished these two subgroups with 100% sensitivity and 88% specificity (92% accuracy). The value of the only grade III meningioma is indicated by the gray circle.

Second, kinetic AMT parameters could differentiate meningiomas from both low-grade gliomas (97% accuracy by k_3'ratios) and high-grade gliomas (83% accuracy by K ratios) (**Figure 9.**). Finally, among 3 initial KP enzymes (IDO1, IDO2, and TDO2), TDO2 showed the strongest immunostaining, particularly in grade I meningiomas (**Figure 10.**). TDO2 also showed a strong negative correlation with AMT k_3'ratios ($p = 0.001$).

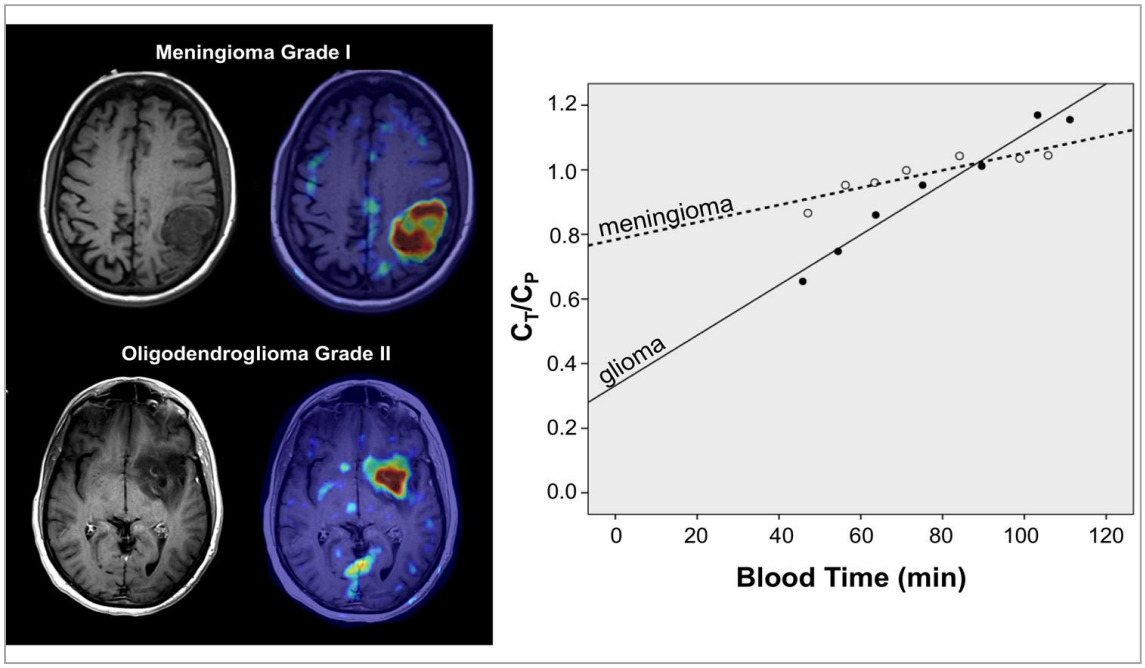

Figure 9. AMT-PET summed images and corresponding Patlak curves of a meningioma and a low-grade glioma. Both tumors showed high AMT standardized uptake values but very different AMT kinetics. The slope of the glioma curve was much steeper than the meningioma curve, indicating higher K value. In contrast, the y intercept was much lower in the glioma, indicating lower volume of distribution (VD′). The x axis represents transformed time ("blood time") in minutes. C_T=tracer concentration in tumor tissue; Cp=tracer concentration in plasma.

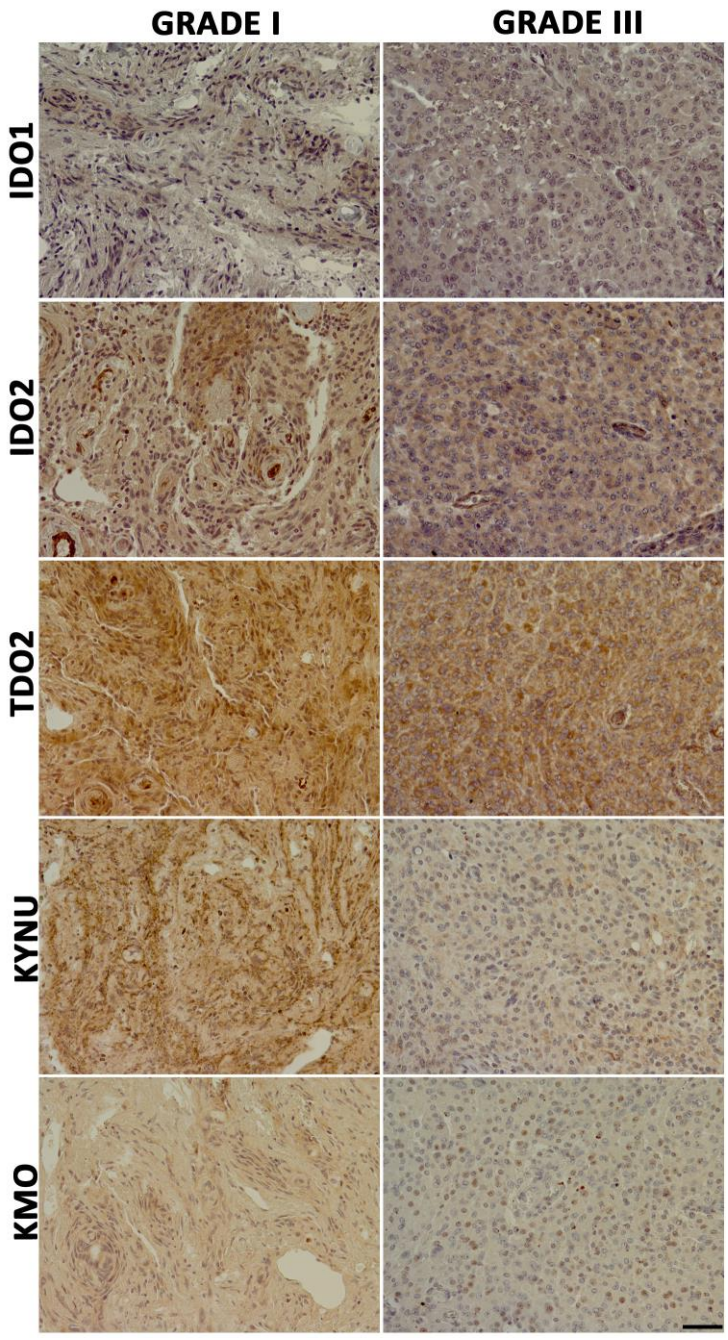

Figure 10. Immunostaining for five key enzymes of the kynurenine pathway in a grade I and a grade III meningioma. For the initial rate-limiting enzymes, both tumors showed TDO2>IDO2>IDO1 immunostaining. Between the two downstream enzymes, KYNU showed stronger staining as compared to KMO. The grade III meningioma showed an overall weaker immunostaining for the same enzymes as compared to the grade I tumor. Original magnification is 20×. The length of the scale bar is 50 μm and applies to all images.

V. DISCUSSION

V.1. *Study 1.*

This is the first study to report a link between prognostic genetic glioma biomarkers and tumoral amino acid uptake in glioblastomas. In a GBM group with IDH1 wild-type glioblastomas, MGMT promoter methylation was associated with lower AMT-PET-based metabolic volumes and K-ratios. This correlation suggests that MGMT promoter methylation may affect tumoral amino acid metabolism that can be captured by PET imaging. In addition, EGFR amplification was associated with lower T1-Gad/PET and lower T1-Gad/T2 volume ratios. This finding is consistent with the notion that EGFR amplification leads to EGFR overexpression that promotes angiogenesis and aggressive tumor growth leading to glioma cell infiltration [Furnari et al., 2015]. Low T1-Gad/T2 ratio in EGFR-amplified glioblastomas is consistent with infiltrative edema as a result of enhanced angiogenesis and tumor cell invasion in the non-contrast-enhancing brain [Aghi et al., 2005]. Our data also demonstrate larger relative areas with high tryptophan uptake beyond the contrast-enhancing tumor mass in EGFR-amplified glioblastomas. Increased amino acid uptake outside the contrast-enhancing tumor mass can mark glioma cell infiltration, as demonstrated by previous studies employing PET-image guided biopsy.

Our second major finding in this study is that high AMT tumor/cortex uptake ratio was a strong prognostic imaging marker associated with a markedly longer survival in this patient group. This was an unexpected finding, as previous amino acid PET studies demonstrated a correlation between high tracer uptake and shorter survival [Kim et al., 2005; Galldiks et al., 2012; Kobayashi et al., 2015; Yoo et al., 2015]. This difference

could be potentially explained by several factors, including the differences in the studied tumor populations and the different metabolic pathways of AMT vs. other amino acid PET tracers in the tumor microenvironment (see further details in Bosnyák et al., 2017).

Altogether, our data demonstrate specific MRI and AMT-PET characteristics associated with prognostic molecular markers in IDH1 wild-type glioblastoma. Importantly, high AMT uptake ratios on PET were found to be a robust prognostic imaging marker, regardless of other, molecular or clinical prognostic factors. Therefore, molecular imaging of tryptophan metabolism is worth further studies for prognostic imaging in patients with newly-diagnosed glioblastoma.

V.2. *Study 2.*

Malignant gliomas show high tryptophan uptake on PET imaging [Juhász et al., 2006; 2014; Kamson et al., 2013]. In this study we demonstrated that amino acid PET imaging with AMT could complement conventional contrast-enhanced MRI not only for detecting glioma recurrence but also predicting the location and timing of subsequent tumor progression. We found that high tryptophan uptake in post-treatment gliomas commonly extends beyond the MRI contrast-enhancing area suspicious for tumor recurrence. Also, subsequent progression of the contrast-enhancing area filled the originally contrast negative, but PET+ area and in many cases, extended beyond this area. Thus, this PET+ but MRI contrast negative areas indicate brain regions at high risk for tumor progression.

Another major finding of this study is the negative correlation between the AMT SUV and time to T1-Gad MRI progression, indicating that higher AMT uptake in non-

enhancing areas could predict earlier glioma progression. Patients with AMT SUV_{max} above 4 showed an early tumor progression (within 5 months), while patients with $SUV_{max}<4$ stayed stable or had late progression (during 2-year follow-up). Thus, AMT SUV_{max} could be an imaging biomarker for imminent tumor progression, which may prompt more frequent MRI follow-up or targeted interventions.

Despite these encouraging results, our study has some inherent limitations, such as the small study population; therefore, the findings will need further confirmation in a larger cohort of patients. In the future, larger, prospective studies could refine the role of amino acid PET imaging in subgroups showing various patterns of MRI progression and also could help optimize cutoff thresholds and test if other amino acid PET tracers provide similar or better results.

V.3. Study 3.

This is the first study to assess imaging correlates of cerebral tryptophan metabolism in brain tumor-associated depression. We found a high rate of depression in our group of patients with a variety of brain tumors, who were not diagnosed and treated before for depression. Higher depression scores were related to variations in tryptophan kinetic variables in several cortical and subcortical structures contralateral to the tumors in brain regions showing no apparent MRI abnormalities.

Our findings demonstrated that abnormalities of tryptophan transport and metabolism in the thalamus, striatum, and frontal cortex, measured by PET, are associated with depression in patients with brain tumor. Specifically, depressed patients showed higher

AMT VD values (suggesting higher tryptophan transport) in the frontal cortex and striatum, two key components of the fronto-striatal network, previously implicated in depressive symptoms [Furman et al., 2011]. These findings may suggest an imbalance between tryptophan metabolism via the serotonin and kynurenine pathways, which may play a role in tumor-associated depression. Altered tryptophan metabolism in non-tumoral brain, measured by PET, may be a novel imaging marker of brain tumor-associated depression.

Several FDG-PET studies showed depression-related variations in brain structures similar to the structures detected in our present study, including fronto-temporal cortices and the basal ganglia [Tashiro et al., 2000; 2001; Inagaki et al., 2007; Kumano et al., 2007]. Also consistent with this, FDG-PET studies performed in patients with major depressive disorder (not associated with cancer) showed decreased brain metabolism in similar brain regions, including the prefrontal cortex, basal ganglia, and temporo-parietal cortices [Baxter et al., 1989; Drevets et al., 1997]. Overall, these data strongly suggest that the main neural substrates of depression are similar in cancer patients and those with major depression. The above mentioned structures, showing metabolic changes in depressed patients, are parts of specific brain circuits that play a role in depressive symptoms, such as the fronto-striatal and limbic circuits.

One concern with the use of the BDI-II in subjects with a somatic disease is that the total score may, at least partially, reflect the disease severity rather than clinical depression. In our study, an exploratory analysis showed that the somatic subscale scores had the strongest correlation with thalamic AMT uptake, while the cognitive-affective scores also

correlated with fronto-striatal tryptophan kinetic variables (data not shown in the manuscript).

This study has some limitations, such as small number of patients; therefore, potential tumor-type-specific effects could not be completely excluded (although major effects were not detected). Also, our analysis was confined to a limited number of brain regions and did not include some potentially relevant structures, such as the amygdala.

Despite these limitations, our findings demonstrate that tryptophan transport and metabolism in the thalamus, striatum, and fronto-temporal cortex are associated with depression in patients with a brain tumor. The observed imaging abnormalities may indicate an imbalance between the serotonin and kynurenine pathways. Altered tryptophan metabolism in non-tumoral brain, measured by PET, may be a novel imaging marker of brain tumor-associated depression.

V.4. *Study 4.*

In this study of meningiomas, the most clinically important finding is the high accuracy of AMT-PET to distinguish grade I versus grade II-III meningiomas. This accuracy seems to be better than the differentiating accuracy reported for MET-PET. For example, Arita et al. did not find any correlation between methionine uptake and proliferative activity, microvessel density, and histological grade [Arita et al., 2012]. We have demonstrated that kinetic analysis of tryptophan uptake by PET can differentiate low-grade versus high-grade meningiomas, which might be useful in optimal clinical management decisions. A second finding is that AMT-PET kinetic parameters showed a striking difference between

meningiomas and both grade II and grade III gliomas. As a result, meningiomas could be differentiated from high-grade gliomas with 83% accuracy; the accuracy was even higher for low-grade gliomas (97%), although these are rarely mistaken for meningiomas. While most meningiomas can be reliably identified on conventional MRI, up to 15% follow an atypical pattern [Buetow et al., 1991; Harting et al., 2004]. These morphological features can mimic a malignant glioma with necrotic changes. Thus, AMT-PET kinetic analysis may supplement MRI in selected cases to establish tumor type before treatment. The exact processes underlying the striking difference in tryptophan kinetics in meningiomas versus gliomas remain unclear, but there are several potential mechanisms (see details in Bosnyák et al., 2015).

In addition, the presence of multiple KP enzymes in grade I-III meningiomas supports the opportunity of pharmacological targeting of the KP, including TDO2, which appears to play a role (in addition to IDO1 and IDO2) in abnormal tryptophan metabolism in meningiomas. The preferential expression of TDO2 in meningiomas is a novel finding that certainly deserves further attention. In previous studies, TDO2 was found to be expressed in malignant gliomas, with or without co-expression of IDO1 or IDO2 [Opitz et al., 2011]. Our results suggest that TDO2 may play a key role in conversion of tryptophan to kynurenine and downstream metabolites in meningiomas, potentially contributing to tumor-induced immunosuppression. Future studies are warranted to determine the role and effect of the KP enzymes in meningioma immune tolerance and tumor proliferation. Molecular imaging with AMT or other radiotracers targeting the KP could be instrumental for monitoring in vivo treatment effects in future clinical trials with KP enzyme inhibitors.

VI. Summary

New Findings:

- We have detected link between prognostic genetic glioma biomarkers (such as IDH, MGMT, EGFR) and tumoral amino acid uptake in glioblastomas. Specific MRI and AMT-PET characteristics associated with prognostic molecular markers in IDH1 wild-type glioblastoma.
- High AMT tumor/cortex uptake ratio was a strong prognostic imaging marker associated with a markedly longer survival in primary (IDH1 wild-type) glioblastomas.
- AMT-PET could complement conventional contrast-enhanced MRI not only for detecting glioma recurrence but also predicting the location and timing of subsequent tumor progression.
- Negative correlation between the AMT SUV and time to T1-Gad MRI progression, indicating that higher AMT uptake in non-enhancing peritumoral areas could predict earlier glioma progression.
- Link has been found between imaging of cerebral tryptophan metabolism in brain tumor-associated depression. Abnormalities of tryptophan transport and metabolism in the thalamus, striatum, and frontal cortex, measured by PET, are associated with depression in patients with brain tumor.
- AMT-PET is able to distinguish grade I versus grade II-III meningiomas with high accuracy.

- AMT-PET kinetic parameters also showed a striking difference between meningiomas and both grade II and grade III gliomas. Meningiomas could be differentiated from high-grade gliomas with 83% accuracy and with 97% accuracy from low-grade gliomas using AMT-PET.

My studies have built upon previous observations demonstrating that AMT-PET is useful in evaluation of various brain tumors. The four studies summarized above included a diverse group of brain tumors and described several novel, previously unexplored clinical applications of this PET modality in both pre- and post-treatment assessments. These studies illustrate the versatility of tryptophan PET imaging and also highlight the additional information we can derive from tracer kinetic analysis and multi-modality imaging by combining quantitative PET and MRI variables. The results provided proof-of-principle data for the potential utility of this imaging approach to assess molecular characteristics of various brain tumors, obtain objective prognostic biomarkers, and understand potential mechanisms of tumor-associated depression. In a preliminary study, we have also recently demonstrated the ability of AMT-PET to monitor the early treatment response to Tumor-Treating Fields therapy in recurrent glioblastoma (Bosnyák et al., 2017). While these data are very promising, it should be noted that AMT-PET is not widely used in clinical radiology mostly because of the short half-life of C-11 (20 min). In order to overcome this limitation, there have been recent efforts to develop novel, F-18 labeled tryptophan analogs, to image tryptophan transport and metabolism via the kynurenine pathway. The initial results are promising, e.g., with the synthesis of 1-(2-^{18}-fluoroethyl)-L-tryptophan [Henrottin et al., 2016; Xin & Cai, 2017], which showed robust

tumor uptake and kinetics similar to AMT in patient-derived xenograft models [Michelhaugh et al., 2017]. The favorable clinical results with AMT-PET, outlined in this thesis, will provide the motivation for further work in this field toward improved, clinically feasible molecular imaging methods for the evaluation of metabolism of tryptophan (and other amino acids) in human cancers. Further multimodal studies incorporating advanced, quantitative MRI with PET imaging are also expected to improve pre- and post-treatment assessment of brain tumors in the near future.

VII. REFERENCES

Aghi M, Gaviani P, Henson JW, Batchelor TT, Louis DN, Barker FG 2nd. Magnetic resonance imaging characteristics predict epidermal growth factor receptor amplification status in glioblastoma. Clin Cancer Res. 2005; 11:8600-8605.

Agnihotri S, Burrell KE, Wolf A, Jalali S, Hawkins C, Rutka JT, Zadeh G. Glioblastoma, a brief review of history, molecular genetics, animal models and novel therapeutic strategies. Arch Immunol Ther Exp (Warsz). 2013; 61:25–41.

Alkonyi B, Barger GR, Mittal S, Muzik O, Chugani DC, Bahl G, Robinette NL, Kupsky WJ, Chakraborty PK, Juhász C. Accurate differentiation of recurrent gliomas from radiation injury by kinetic analysis of α-^{11}C-methyl-L-tryptophan PET. J Nucl Med. 2012; 53:1058-1064.

Alkonyi B, Mittal S, Zitron I, Chugani DC, Kupsky WJ, Muzik O, Chugani HT, Sood S, Juhász C. Increased tryptophan transport in epileptogenic dysembryoplastic neuroepithelial tumors. J Neurooncol. 2012; 107:365-72.

Al-Okaili RN, Krejza J, Wang S, Woo JH, Melhem ER. Advanced MR imaging techniques in the diagnosis of intraaxial brain tumors in adults. Radiographics. 2006; 26 Suppl 1:S173-189.

Appin CL, Brat DJ. Molecular genetics of gliomas. Cancer J. 2014; 20:66-72.

Arita H, Kinoshita M, Okita Y, Hirayama R, Watabe T, Ishohashi K, Kijima N, Kagawa N, Fujimoto Y, Kishima H, Shimosegawa E, Hatazawa J, Hashimoto N, Yoshimine T. Clinical characteristics of meningiomas assessed by ^{11}C-methionine and ^{18}F-fluorodeoxy glucose positron-emission tomography. J Neurooncol. 2012; 107:379–386.

Arnold SM, Patchell RA. Diagnosis and management of brain metastases. Hematol Oncol Clin North Am. 2001; 15:1085–1107

Austin CJ, Rendina LM. Targeting key dioxygenases in tryptophan-kynurenine metabolism for immunomodulation and cancer chemotherapy. Drug Discov Today. 2014. pii:S1359-6446(14)00444-9.

Barajas RF Jr, Hodgson JG, Chang JS, Vandenberg SR, Yeh RF, Parsa AT, McDermott MW, Berger MS, Dillon WP, Cha S. Glioblastoma multiforme regional genetic and cellular expression patterns: influence on anatomic and physiologic MR imaging. Radiology. 2010; 254:564–576.

Bartelt S, Lutterbach J. Brain metastases in patients with cancer of unknown primary. J Neurooncol. 2003; 64:249-53.

Batista CE, Juhasz C, Muzik O, Kupsky WJ, barger G, Chugani HT, Mittal S, Sood S, Chakraborty PK, Chugani DC. Imaging correlates of differential expression of indoleamine 2,3-dioxygenase in human brain tumors. Mol Imaging Biol. 2009; 11:460-466.

Baxter Jr LR, Schwartz JM, Phelps ME, Mazziotta JC, Guze BH, Selin CE, Gerner RH, Sumida RM. Reduction of prefrontal cortex glucose metabolism common to three types of depression. Arch Gen Psychiatry. 1989; 46:243–250.

Becherer A, Karanikas G, Szabó M, Zettinig G, Asenbaum S, Marosi C, Henk C, Wunderbaldinger P, Czech T, Wadsak W, Kletter K. Brain tumour imaging with PET: a comparison between [^{18}F]fluorodopa and [^{11}C]methionine. Eur J Nucl Med Mol Imaging. 2003; 30:1561–1567.

Beck ATS, Steer RA, Brown GK. Manual for The Beck Depression Inventory Second Edition (BDI-II). San Antonio: Psychological Corporation; 1996.

Belden CJ, Valdes PA, Ran C, Pastel DA, Harris BT, Fadul CE, Israel MA, Paulsen K, Roberts DW. Genetics of glioblastoma: a window into its imaging and histopathologic variability. Radiographics. 2011; 31:1717–1740.

Bi WL, Mei Y, Agarwalla PK, Beroukhim R, Dunn IF. Genomic and epigenomic landscape in meningioma. Neurosurg Clin North Am. 2016; 27:167–179.

Bosnyák E, Kamson DO, Guastella AR, Varadarajan K, Robinette NL, Kupsky WJ, Muzik O, Michelhaugh SK, Mittal S, Juhász C. Molecular imaging correlates of tryptophan metabolism via the kynurenine pathway in human meningiomas. Neuro Oncol. 2015; 17:1284-1292.

Bosnyák E, Michelhaugh SK, Klinger NV, Kamson DO, Barger GR, Mittal S, Juhász C. Prognostic Molecular and Imaging Biomarkers in Primary Glioblastoma. Clin Nucl Med. 2017; 42:341-347.

Bosnyák E, Barger GR, Michelhaugh SK, Robinette NL, Amit-Yousif A, Mittal S, Juhász C. Amino Acid PET Imaging of the Early Metabolic Response during Tumor-Treating Fields (TTFields) Therapy in recurrent Glioblastoma. Clin Nucl Med. 2018; 43:176-179.

Brastianos PK, Horowitz PM, Santagata S, Jones RT, McKenna A, Getz G, Ligon KL, Palescandolo E, Van Hummelen P, Ducar MD, Raza A, Sunkavalli A, Macconaill LE, Stemmer-Rachamimov AO, Louis DN, Hahn WC, Dunn IF, Beroukhim R. Genomic sequencing of meningiomas identifies oncogenic SMO and AKT1 mutations. Nat Genet. 2013; 45:285–289.

Brandsma D, Stalpers L, Taal W, Sminia P, van den Bent MJ. Clinical features, mechanisms, and management of pseudoprogression in malignant gliomas. Lancet Oncol. 2008; 9:453–461.

Bruzzone MG, D'Incerti L, Farina LL, Cuccarini V, Finocchiaro G. CT and MRI of brain tumors. Q J Nucl Med Mol Imaging. 2012; 56:112-137.

Brenner AV, Linet MS, Fine HA, Shapiro WR, Selker RG, Black PM, Inskip PD. History of allergies and autoimmune diseases and risk of brain tumors in adults. Int J Cancer. 2002; 99:252–259.

Buetow MP, Buetow PC, Smirniotopoulos JG. Typical, atypical, and misleading features in meningioma. Radiographics. 1991; 11:1087–1106.

Cancer Genome Atlas Research Network. Comprehensive genomic characterization defines human glioblastoma genes and core pathways. Nature. 2008; 455:1061-1068.

Cancer Genome Atlas Research Network, Brat DJ, Verhaak RG, Aldape KD, Yung WK, Salama SR, Cooper LA, Rheinbay E, Miller CR, Vitucci M, Morozova O, Robertson AG, Noushmehr H, Laird PW, Cherniack AD, Akbani R, Huse JT, Ciriello G, Poisson LM, Barnholtz-Sloan JS, Berger MS, Brennan C, Colen RR, Colman H, Flanders AE, Giannini C, Grifford M, Iavarone A, Jain R, Joseph I, Kim J, Kasaian K, Mikkelsen T, Murray BA, O'Neill BP, Pachter L, Parsons DW, Sougnez C, Sulman EP, Vandenberg SR, Van Meir EG, von Deimling A, Zhang H, Crain D, Lau K, Mallery D, Morris S, Paulauskis J, Penny R, Shelton T, Sherman M, Yena P, Black A, Bowen J, Dicostanzo K, Gastier-Foster J, Leraas KM, Lichtenberg TM, Pierson CR, Ramirez NC, Taylor C, Weaver S, Wise L, Zmuda E, Davidsen T, Demchok JA, Eley G, Ferguson ML, Hutter CM, Mills Shaw KR, Ozenberger BA, Sheth M, Sofia HJ, Tarnuzzer R, Wang Z, Yang L, Zenklusen JC, Ayala B, Baboud J, Chudamani S, Jensen MA, Liu J, Pihl T, Raman R, Wan Y, Wu Y, Ally A, Auman JT, Balasundaram M, Balu S, Baylin SB, Beroukhim R, Bootwalla MS, Bowlby R, Bristow CA, Brooks D, Butterfield Y, Carlsen R, Carter S, Chin L, Chu A, Chuah E, Cibulskis K, Clarke A, Coetzee SG, Dhalla N, Fennell T, Fisher S, Gabriel S, Getz G, Gibbs R, Guin R, Hadjipanayis A, Hayes DN, Hinoue T, Hoadley K, Holt RA, Hoyle AP, Jefferys SR, Jones S, Jones CD, Kucherlapati R, Lai PH, Lander E, Lee S, Lichtenstein L, Ma Y, Maglinte DT, Mahadeshwar HS, Marra MA, Mayo M, Meng S, Meyerson ML, Mieczkowski PA, Moore RA, Mose LE, Mungall AJ, Pantazi A, Parfenov M, Park PJ, Parker JS, Perou CM, Protopopov A, Ren X, Roach J, Sabedot TS, Schein J, Schumacher SE, Seidman JG, Seth S, Shen H, Simons JV, Sipahimalani P, Soloway MG, Song X, Sun H, Tabak B, Tam A, Tan D, Tang J, Thiessen N, Triche T Jr, Van Den Berg DJ, Veluvolu U, Waring S, Weisenberger DJ, Wilkerson MD, Wong T, Wu J, Xi L, Xu AW, Yang L, Zack TI, Zhang J, Aksoy BA, Arachchi H, Benz C, Bernard B, Carlin D, Cho J, DiCara D, Frazer S, Fuller GN, Gao J, Gehlenborg N, Haussler D, Heiman DI, Iype L, Jacobsen A, Ju Z, Katzman S, Kim H, Knijnenburg T, Kreisberg RB, Lawrence MS, Lee W, Leinonen K, Lin P, Ling S, Liu W, Liu Y, Liu Y, Lu Y, Mills G, Ng S, Noble MS, Paull E, Rao A, Reynolds S, Saksena G, Sanborn Z, Sander C, Schultz N, Senbabaoglu Y, Shen R, Shmulevich I, Sinha R, Stuart J, Sumer SO, Sun Y, Tasman N, Taylor BS, Voet D, Weinhold N, Weinstein JN, Yang D, Yoshihara K, Zheng S, Zhang W, Zou L, Abel T, Sadeghi S, Cohen ML, Eschbacher J, Hattab EM, Raghunathan A, Schniederjan MJ, Aziz D, Barnett G, Barrett W, Bigner DD, Boice L, Brewer C, Calatozzolo C, Campos B, Carlotti CG Jr, Chan TA, Cuppini L, Curley E, Cuzzubbo S, Devine K, DiMeco F, Duell R, Elder JB, Fehrenbach A, Finocchiaro G, Friedman W, Fulop J, Gardner J, Hermes B, Herold-Mende C, Jungk C, Kendler A, Lehman NL, Lipp E, Liu O, Mandt R, McGraw M, Mclendon R, McPherson C, Neder L, Nguyen P, Noss A, Nunziata R, Ostrom QT, Palmer C, Perin A, Pollo B, Potapov A, Potapova O, Rathmell

WK, Rotin D, Scarpace L, Schilero C, Senecal K, Shimmel K, Shurkhay V, Sifri S, Singh R, Sloan AE, Smolenski K, Staugaitis SM, Steele R, Thorne L, Tirapelli DP, Unterberg A, Vallurupalli M, Wang Y, Warnick R, Williams F, Wolinsky Y, Bell S, Rosenberg M, Stewart C, Huang F, Grimsby JL, Radenbaugh AJ, Zhang J. Comprehensive, integrative genomic analysis of diffuse lower-grade gliomas. N Engl J Med. 2015; 372:2481–2498.

Castellano A, Falini A. Progress in neuro-imaging of brain tumors. Curr Opin Oncol. 2016; 28:484-493.

Cha S. Neuroimaging in neuro-oncology. Neurotherapeutics. 2009; 6:465-477.

Chakraborty PK, Mangner TJ, Chugani DC, Muzik O, Chugani HT. A high-yield and simplified procedure for the synthesis of alpha-[^{11}C]methyl-L-tryptophan. Nucl Med Biol. 1996; 23:1005–1008.

Chen W, Silverman DH, Delaloye S, Czernin J, Kamdar N, Pope W, Satyamurthy N, Schiepers C, Cloughesy T. ^{18}F-FDOPA PET imaging of brain tumors: comparison study with ^{18}F-FDG PET and evaluation of diagnostic accuracy. J Nucl Med. 2006; 47:904–911.

Chugani DC, Chugani HT, Muzik O, Shah JR, Shah AK, Canady A, Mangner TJ, Chakraborty PK. Imaging epileptogenic tubers in children with tuberous sclerosis complex using alpha-[^{11}C]methyl-L-tryptophan positron emission tomography. Ann Neurol. 1998; 44:858-66.

Chugani DC, Muzik O. Alpha[C-11]methyl-L-tryptophan PET maps brain serotonin synthesis and kynurenine pathway metabolism. J Cereb Blood Flow Metab. 2000; 20:2–9.

Claus EB, Bondy ML, Schildkraut JM, Wiemels JL, Wrensch M, Black PM. Epidemiology of intracranial meningioma. Neurosurgery 2005; 57:1088–1095.

de Blank PM, Ostrom QT, Rouse C, Wolinsky Y, Kruchko C, Salcido J, Barnholtz-Sloan JS. Years of life lived with disease and years of potential life lost in children who die of cancer in the United States, 2009. Cancer Med. 2015; 4:608–619.

Delgado-López PD, Corrales-García EM. Survival in glioblastoma: a review on the impact of treatment modalities. Clin Transl Oncol. 2016; 18:1062-1071.

Dhermain FG, Hau P, Lanfermann H, Jacobs AH, van den Bent MJ. Advanced MRI and PET imaging for assessment of treatment response in patients with gliomas. Lancet Neurol. 2010; 9:906-920.

Diksic M, Nagahiro S, Sourkes TL, Yamamoto YL. A new method to measure brain serotonin synthesis in vivo. I. Theory and basic data for a biological model. J Cereb Blood Flow Metab. 1990; 10:1–12.

Diksic M, Nagahiro S, Chaly T, Sourkes TL, Yamamoto YL, Feindel W. Serotonin synthesis rate measured in living dog brain by positron emission tomography. J Neurochem. 1991; 56:153–162.

Dozois DJA, Dobson KS, Ahnberg JL. A psychometric evaluation of the Beck Depression Inventory - II. Psychol Assessment. 1998; 10:83–89.

Drevets WC, Price JL, Simpson Jr JR, Todd RD, Reich T, Vannier M, Raichle ME. Subgenual prefrontal cortex abnormalities in mood disorders. Nature. 1997; 386:824–827.

Dunet V, Rossier C, Buck A, Stupp R, Prior JO. Performance of ^{18}F-fluoro-ethyl-tyrosine (^{18}F-FET) PET for the differential diagnosis of primary brain tumor: a systematic review and metaanalysis. J Nucl Med. 2012; 53:207–214.

Eckel-Passow JE, Lachance DH, Molinaro AM, Walsh KM, Decker PA, Sicotte H, Pekmezci M, Rice T, Kosel ML, Smirnov IV, Sarkar G, Caron AA, Kollmeyer TM, Praska CE, Chada AR, Halder C, Hansen HM, McCoy LS, Bracci PM, Marshall R, Zheng S, Reis GF, Pico AR, O'Neill BP, Buckner JC, Giannini C, Huse JT, Perry A, Tihan T, Berger MS, Chang SM, Prados MD, Wiemels J, Wiencke JK, Wrensch MR, Jenkins RB. Glioma Groups Based on 1p/19q, IDH, and TERT Promoter Mutations in Tumors. N Engl J Med. 2015; 372:2499-2508.

Eidelberg D, Takikawa S, Dhawan V, Chaly T, Robeson W, Dahl R, Margouleff D, Moeller JR, Patlak CS, Fahn S. Striatal ^{18}F-DOPA uptake: absence of an aging effect. J Cereb Blood Flow Metab. 1993; 13:881–888.

Eisele SC, Wen PY, Lee EQ. Assessment of Brain Tumor Response: RANO and Its Offspring. Curr Treat Options Oncol. 2016; 17:35.

ElBanan MG, Amer AM, Zinn PO, Colen RR. Imaging genomics of Glioblastoma: state of the art bridge between genomics and neuroradiology. Neuroimaging Clin N Am. 2015; 25:141-153.

Erdélyi-Bótor S, Komáromy H, Kamson DO, Kovács N, Perlaki G, Orsi G, Molnár T, Illes Z, Nagy L, Kéki S, Deli G, Bosnyák E, Trauninger A, Pfund Z. Serum L-arginine and dimethylarginine levels in migraine patients with brain white matter lesions. Cephalalgia. 2017; 37:571-580.

Fisher JL, Schwartzbaum JA, Wrensch M, Wiemels JL. Epidemiology of brain tumors. Neurol Clin. 2007; 25:867-890.

Friedman HS, Prados MD, Wen PY, Mikkelsen T, Schiff D, Abrey LE, Yung WK, Paleologos N, Nicholas MK, Jensen R, Vredenburgh J, Huang J, Zheng M, Cloughesy T. Bevacizumab Alone and in Combination With Irinotecan in Recurrent Glioblastoma. J Clin Oncol. 2009; 27:4733–4740.

Fueger BJ, Czernin J, Cloughesy T, Silverman DH, Geist CL, Walter MA, Schiepers C, Nghiemphu P, Lai A, Phelps ME, Chen W. Correlation of 6-^{18}F-fluoro-L-dopa PET uptake with proliferation and tumor grade in newly diagnosed and recurrent gliomas. J Nucl Med. 2010; 51:1532–1538.

Furman DJ, Hamilton JP, Gotlib IH. Frontostriatal functional connectivity in major depressive disorder. Biol Mood Anxiety Disord. 2011; 1:11.

Furnari FB, Cloughesy TF, Cavenee WK, Mischel PS. Heterogeneity of epidermal growth factor receptor signalling networks in glioblastoma. Nat Rev Cancer. 2015; 15:302-310.

Galldiks N, Kracht LW, Dunkl V, Ullrich RT, Vollmar S, Jacobs AH, Fink GR, Schroeter M. Imaging of non- or very subtle contrast-enhancing malignant gliomas with [^{11}C]-methionine positron emission tomography. Mol Imaging. 2011; 10:453–459.

Galldiks N, Dunkl V, Kracht LW, Vollmar S, Jacobs AH, Fink GR, Schroeter M. Volumetry of [^{11}C]-methionine positron emission tomographic uptake as a prognostic marker before treatment of patients with malignant glioma. Mol Imaging. 2012; 11:516-527.

Glaudemans AW, Enting RH, Heesters MA, Dierckx RA, van Rheenen RW, Walenkamp AM, Slart RH. Value of ^{11}C-methionine PET in imaging brain tumours and metastases. Eur J Nucl Med Mol Imaging. 2013; 40:615–635.

Goebel S, Mehdorn HM. Development of anxiety and depression in patients with benign intracranial meningiomas: a prospective long-term study. Support Care Cancer. 2013; 21:1365–1372.

Goldbrunner R, Minniti G, Preusser M, Jenkinson MD, Sallabanda K, Houdart E, von Deimling A, Stavrinou P, Lefranc F, Lund-Johansen M, Moyal EC, Brandsma D, Henriksson R, Soffietti R, Weller M. EANO guidelines for the diagnosis and treatment of meningiomas. Lancet Oncol. 2016; 17:e383-391.

Gonzalez-Martinez JA, Najm IM. Meningiomas and epilepsy. In: Lee JH (ed) Meningiomas: diagnosis, treatment, and outcome. Springer, London. 2008; pp 243–246.

Gotz I, Grosu AL. [^{18}F]FET-PET imaging for treatment and response monitoring of radiation therapy in malignant glioma patients - a review. Front Oncol. 2013; 3:104.

Goutagny S, Nault JC, Mallet M, Henin D, Rossi JZ, Kalamarides M. High incidence of activating TERT promoter mutations in meningiomas undergoing malignant progression. Brain Pathol. 2014; 24:184–189.

Gulyas B, Halldin C. New PET radiopharmaceuticals beyond FDG for brain tumor imaging. Q J Nucl Med Mol Imaging. 2012; 56:173–190.

Haining Z, Kawai N, Miyake K, Okada M, Okubo S, Zhang X, Fei Z, Tamiya T. Relation of LAT1/4F2hc expression with pathological grade, proliferation and angiogenesis in human gliomas. BMC Clin Pathol. 2012; 12:4.

Hall WA, Djalilian HR, Nussbaum ES, Cho KH. Long-term survival with metastatic cancer to the brain. Med Oncol. 2000; 17:279-286.

Hamasaki T, Yamada K, Yano S, Nakamura H, Makino K, Hide T, Hasegawa Y, Kuroda J, Hirai T, Kuratsu J. Higher incidence of epilepsy in meningiomas located on the premotor cortex: a voxel-wise statistical analysis. Acta Neurochir (Wien). 2012; 154:2241-2249.

Harting I, Hartmann M, Bonsanto MM, Sommer C, Sartor K. Characterization of necrotic meningioma using diffusion MRI, perfusion MRI, and MR spectroscopy: case report and review of the literature. Neuroradiology. 2004; 46:189–193.

Heiss P, Mayer S, Herz M, Wester HJ, Schwaiger M, Senekowitsch-Schmidtke R. Investigation of transport mechanism and uptake kinetics of O-(2-[^{18}F]fluoroethyl)-l-tyrosine in vitro and in vivo. J Nucl Med. 1999; 40:1367–1373.

Henrottin J, Lemaire C, Egrise D, Zervosen A, Van den Eynde B, Plenevaux A, Franci X, Goldman S, Luxen A. Fully automated radiosynthesis of ^{1}N-[^{18}F]fluoroethyl-tryptophan and study of its biological activity as a new potential substrate for indoleamine 2,3-dioxygenase PET imaging. Nucl Med Biol. 2016; 43:379-389.

Huang C, McConathy J. Radiolabeled amino acids for oncologic imaging. J Nucl Med. 2013; 54:1007–1010.

Imai H, Kaira K, Oriuchi N, Shimizu K, Tominaga H, Yanagitani N, Sunaga N, Ishizuka T, Nagamori S, Promchan K, Nakajima T, Yamamoto N, Mori M, Kanai Y. Inhibition of L-type amino acid transporter 1 has antitumor activity in non-small cell lung cancer. Anticancer Res. 2010; 30:4819–4828.

Inagaki M, Yoshikawa E, Kobayakawa M, Matsuoka Y, Sugawara Y, Nakano T, Akizuki N, Fujimori M, Akechi T, Kinoshita T, Furuse J, Murakami K, Uchitomi Y. Regional cerebral glucose metabolism in patients with secondary depressive episodes after fatal pancreatic cancer diagnosis. J Affect Disord. 2007; 99:231–236.

Jeong JW, Juhász C, Mittal S, Bosnyák E, Kamson DO, Barger GR, Robinette NL, Kupsky WJ, Chugani DC. Multi-modal imaging of tumor cellularity and Tryptophan metabolism in human Gliomas. Cancer Imaging. 2015; 15:10.

Juhász C, Chugani DC, Muzik O, Shah A, Asano E, Mangner TJ, Chakraborty PK, Sood S, Chugani HT. Alpha-methyl-L-tryptophan PET detects epileptogenic cortex in children with intractable epilepsy. Neurology. 2003; 60:960-8.

Juhász C, Chugani DC, Muzik O, Wu D, Sloan AE, Barger G, Watson C, Shah AK, Sood S, Ergun EL, Mangner TJ, Chakraborty PK, Kupsky WJ, Chugani HT. In vivo uptake and metabolism of alpha-[^{11}C]methyl-L-tryptophan in human brain tumors. J Cereb Blood Flow Metab. 2006; 26:345–357.

Juhász C, Muzik O, Lu X, Jahania MS, Soubani AO, Khalaf M, Peng F, Mangner TJ, Chakraborty PK, Chugani DC Quantification of tryptophan transport and metabolism in lung tumors using PET. J Nucl Med. 2009; 50:356-63.

Juhász C, Muzik O, Chugani DC, Chugani HT, Sood S, Chakraborty PK, Barger GR, Mittal S. Differential kinetics of alpha-[^{11}C]methyl-L-tryptophan on PET in low-grade brain tumors. J Neurooncol. 2011; 102:409–415.

Juhász C, Chugani DC, Barger GR, Kupsky WJ, Chakraborty PK, Muzik O, Mittal S Quantitative PET imaging of tryptophan accumulation in gliomas and remote cortex: correlation with tumor proliferative activity. Clin Nucl Med. 2012; 37:838-42

Juhász C, Nahleh Z, Zitron I, Chugani DC, Janabi MZ, Bandyopadhyay S, Ali-Fehmi R, Mangner TJ, Chakraborty PK, Mittal S, Muzik O. Tryptophan metabolism in breast cancers: molecular imaging and immunohistochemistry studies. Nucl Med Biol. 2012; 39:926-932.

Juhász C, Dwivedi S, Kamson DO, Michelhaugh SK, Mittal S. Comparison of amino acid positron emission tomographic radiotracers for molecular imaging of primary and metastatic brain tumors. Mol Imaging. 2014; 13.

Juhász C, Bosnyák E. PET and SPECT studies in children with hemispheric low-grade gliomas. Childs Nerv Syst. 2016; 32:1823-32.

Kamson DO, Juhász C, Buth A, Kupsky WJ, Barger GR. Tryptophan PET in pretreatment delineation of newly-diagnosed gliomas: MRI and histopathologic correlates. J Neurooncol. 2013; 112:121-132.

Kamson DO, Mittal S, Buth A, Muzik O, Kupsky WJ, Robinette NL, Barger GR, Juhász C. Differentiation of glioblastomas from metastatic brain tumors by tryptophan uptake and kinetic analysis: a positron emission tomographic study with magnetic resonance imaging comparison. Mol Imaging. 2013; 12:327-337.

Kamson DO, Mittal S, Robinette NL, Muzik O, Kupsky WJ, Barger GR, Juhász C. Increased tryptophan uptake on PET has strong independent prognostic value in patients with a previously treated high-grade glioma. Neuro Oncol. 2014; 16:1373–1383.

Kikinis R, Pieper S. 3D Slicer as a tool for interactive brain tumor segmentation. Conf Proc IEEE Eng Med Biol Soc. 2011; 2011:6982–6984.

Kim S, Chung JK, Im SH, Jeong JM, Lee DS, Kim DG, Jung HW, Lee MC. ^{11}C-methionine PET as a prognostic marker in patients with glioma: comparison with ^{18}F-FDG PET. Eur J Nucl Med Mol Imaging. 2005; 32:52-59.

Kirson ED, Gurvich Z, Schneiderman R, Dekel E, Itzhaki A, Wasserman Y, Schatzberger R, Palti Y. Disruption of cancer cell replication by alternating electric fields. Cancer Res. 2004; 64:3288-3295.

Kirson ED, Dbalý V, Tovarys F, Vymazal J, Soustiel JF, Itzhaki A, Mordechovich D, Steinberg-Shapira S, Gurvich Z, Schneiderman R, Wasserman Y, Salzberg M, Ryffel B, Goldsher D, Dekel E, Palti Y. Alternating electric fields arrest cell proliferation in animal tumor models and human brain tumors. Proc Natl Acad Sci U S A. 2007; 104:10152-10157.

Kirson ED, Schneiderman RS, Dbalý V, Tovarys F, Vymazal J, Itzhaki A, Mordechovich D, Gurvich Z, Shmueli E, Goldsher D, Wasserman Y, Palti Y. Chemotherapeutic treatment efficacy and sensitivity are increased by adjuvant alternating electric fields (TTFields). BMC Med Phys. 2009; 9:1.

Kobayashi K, Hirata K, Yamaguchi S, Manabe O, Terasaka S, Kobayashi H, Shiga T, Hattori N, Tanaka S, Kuge Y, Tamaki N. Prognostic value of volume-based measurements on 11C-methionine PET in glioma patients. Eur J Nucl Med Mol Imaging. 2015; 42:1071-1080.

Koelsche C, Sahm F, Capper D, Reuss D, Sturm D, Jones DT, Kool M, Northcott PA, Wiestler B, Böhmer K, Meyer J, Mawrin C, Hartmann C, Mittelbronn M, Platten M, Brokinkel B, Seiz M, Herold-Mende C, Unterberg A, Schittenhelm J, Weller M, Pfister S, Wick W, Korshunov A, von Deimling A. Distribution of TERT promoter mutations in pediatric and adult tumors of the nervous system. Acta Neuropathol. 2013; 126:907–915.

Kreisl TN, Kim L, Moore K, Duic P, Royce C, Stroud I, Garren N, Mackey M, Butman JA, Camphausen K, Park J, Albert PS, Fine HA. Phase II Trial of Single-Agent Bevacizumab Followed by Bevacizumab Plus Irinotecan at Tumor Progression in Recurrent Glioblastoma. J Clin Oncol. 2009; 27:740–745.

Kumano H, Ida I, Oshima A, Takahashi K, Yuuki N, Amanuma M, Oriuchi N, Endo K, Matsuda H, Mikuni M. Brain metabolic changes associated with predispotion to onset of major depressive disorder and adjustment disorder in cancer patients–a preliminary PET study. J Psychiatr Res. 2007; 41:591–599.

Law M, Yang S, Babb JS, Knopp EA, Golfinos JG, Zagzag D, Johnson G. Comparison of cerebral blood volume and vascular permeability from dynamic susceptibility contrast-enhanced perfusion MR imaging with glioma grade. AJNR Am J Neuroradiol. 2004; 25:746–755.

Law M. Advanced imaging techniques in brain tumors. Cancer Imaging. 2009; 9: S4-9.

Lee Y, Liu J, Patel S, Cloughesy T, Lai A, Farooqi H, Seligson D, Dong J, Liau L, Becker D, Mischel P, Shams S, Nelson S. Genomic landscape of meningiomas. Brain Pathol. 2010; 20:751-62.

Lieu AS, Howng SL. Intracranial meningiomas and epilepsy: incidence, prognosis and influencing factors. Epilepsy Res. 2000; 38: 45–52

Lin BJ, Chou KN, Kao HW, Lin C, Tsai WC, Feng SW, Lee MS, Hueng DY. Correlation between magnetic resonance imaging grading and pathological grading in meningioma. J Neurosurg. 2014; 121:1201−1208.

Louis DN, Ohgaki H, Wiestler OD, Cavenee WK, Burger PC, Jouvet A, Scheithauer BW, Kleihues P. The 2007 WHO classification of tumours of the central nervous system. Acta Neuropathol. 2007; 114:97−109.

Louis DN, Perry A, Reifenberger G, von Deimling A, Figarella-Branger D, Cavenee WK, Ohgaki H, Wiestler OD, Kleihues P, Ellison DW. The 2016 World Health Organization Classification of Tumors of the Central Nervous System: a summary. Acta Neuropathol. 2016; 131:803-820.

Macdonald DR, Cascino TL, Schold SC, Jr. Cairncross JG. Response criteria for phase II studies of supratentorial malignant glioma. J. Clin. Oncol. 1990; 8:1277–1280.

Madhusoodanan S, Ting MB, Farah T, Ugur U. Psychiatric aspects of brain tumors: A review. World J Psychiatry. 2015; 5:273-285.

Mainio A, Hakko H, Timonen M, Niemela A, Koivukangas J, Rasanen P. Depression in relation to survival among neurosurgical patients with a primary brain tumor: a 5-year follow-up study. Neurosurgery. 2005; 56:1234–1241.

Mattes D, Haynor DR, Vesselle H, Lewellen TK, Eubank W. PET-CT image registration in the chest using free-form deformations. IEEE Trans Med Imaging. 2003; 22:120–128.

Matsubara K, Watabe H, Kumakura Y, Hayashi T, Endres CJ, Minato K, Iida H. Sensitivity of kinetic macro parameters to changes in dopamine synthesis, storage, and metabolism: a simulation study for [^{18}F]FDOPA PET by a model with detailed dopamine pathway. Synapse. 2011; 65:751–762.

McNeill KA. Epidemiology of Brain Tumors. Neurol Clin. 2016; 34:981-998.

Michelhaugh SK, Muzik O, Guastella AR, Klinger NV, Polin LA, Cai H, Xin Y, Mangner TJ, Zhang S, Juhász C, Mittal S. Assessment of tryptophan uptake and kinetics using 1-(2-[^{18}F]fluoroethyl)-L-tryptophan and α-[^{11}C]-methyl-L-tryptophan PET imaging in mice implanted with patient-derived brain tumor xenografts. J Nucl Med. 2017; 58:208-213.

Mitsuka K, Kawataki T, Satoh E, Asahara T, Horikoshi T, Kinouchi H. Expression of indoleamine 2,3-dioxygenase and correlation with pathological malignancy in gliomas. Neurosurgery. 2013; 72:1031–1038.

Mittal S, Klinger NV, Michelhaugh SK, Barger GR, Pannullo SC, Juhász C. Alternating electric tumor treating fields for treatment of glioblastoma: rationale, preclinical, and clinical studies. J Neurosurg. 2017; 24:1-8.

Munn DH, Mellor AL. Indoleamine 2,3-dioxygenase and tumor-induced tolerance. J Clin Invest. 2007; 117:1147-1154.

Nagahiro S, Takada A, Diksic M, Sourkes TL, Missala K, Yamamoto YL. A new method to measure brain serotonin synthesis in vivo. II. A practical autoradiographic method tested in normal and lithium-treated rats. J Cereb Blood Flow Metab. 1990; 10:13-21.

Nihashi T, Dahabreh IJ, Terasawa T. PET in the clinical management of glioma: evidence map. AJR Am J Roentgenol. 2013; 200:W654–660.

Okada H, Weller M, Huang R, Finocchiaro G, Gilbert MR, Wick W, Ellingson BM, Hashimoto N, Pollack IF, Brandes AA, Franceschi E, Herold-Mende C, Nayak L, Panigrahy A, Pope WB, Prins R, Sampson JH, Wen PY, Reardon DA. Immunotherapy response assessment in neuro-oncology: a report of the RANO working group. Lancet Oncol. 2015; 16:e534–542.

Omuro A, DeAngelis LM. Glioblastoma and other malignant gliomas: a clinical review. JAMA. 2013; 310:1842-1850.

Opitz CA, Litzenburger UM, Sahm F, Ott M, Tritschler I, Trump S, Schumacher T, Jestaedt L, Schrenk D, Weller M, Jugold M, Guillemin GJ, Miller CL, Lutz C, Radlwimmer B, Lehmann I, von Deimling A, Wick W, Platten M. An endogenous tumour-promoting ligand of the human aryl hydrocarbon receptor. Nature. 2011; 478:197-203.

Osborn AG, Salzman KL, Barkovich AJ. Diagnostic imaging: brain. Amirsys. 2010.

Ostrom QT, Gittleman H, Farah P, Ondracek A, Chen Y, Wolinsky Y, Stroup NE, Kruchko C, Barnholtz-Sloan JS. CBTRUS statistical report: Primary brain and central nervous system tumors diagnosed in the United States in 2006–2010. Neuro Oncol. 2013; 15:ii1–56.

Ostrom QT, Gittleman H, Liao P, Rouse C, Chen Y, Dowling J, Wolinsky Y, Kruchko C, Barnholtz-Sloan J. CBTRUS statistical report: primary brain and central nervous system tumors diagnosed in the United States in 2007-2011. Neuro Oncol. 2014; 16:iv1-iv63.

Ostrom QT, Gittleman H, Fulop J, Liu M, Blanda R, Kromer C, Wolinsky Y, Kruchko C, Barnholtz-Sloan JS. CBTRUS statistical report: primary brain and central nervous system tumors diagnosed in the United States in 2008–2012. Neuro Oncol. 2015; 17:iv1–62.

Ostrom QT, Gittleman H, Xu J, Kromer C, Wolinsky Y, Kruchko C, Barnholtz-Sloan JS. CBTRUS Statistical Report: Primary Brain and Other Central Nervous System Tumors Diagnosed in the United States in 2009-2013. Neuro-Oncol. 2016; 18:v1-v75.

Pallud J, Fontaine D, Duffau H, Mandonnet E, Sanai N, Taillandier L, Peruzzi P, Guillevin R, Bauchet L, Bernier V, Baron MH, Guyotat J, Capelle L. Natural history of incidental world health organization grade II gliomas. Ann Neurol. 2010; 68:727–733.

Parsons DW, Jones S, Zhang X, Lin JC, Leary RJ, Angenendt P, Mankoo P, Carter H, Siu IM, Gallia GL, Olivi A, McLendon R, Rasheed BA, Keir S, Nikolskaya T, Nikolsky Y, Busam DA, Tekleab H, Diaz LA Jr, Hartigan J, Smith DR, Strausberg RL, Marie SK, Shinjo SM, Yan H, Riggins GJ, Bigner DD, Karchin R, Papadopoulos N, Parmigiani G, Vogelstein B, Velculescu VE, Kinzler KW. An integrated genomic analysis of human glioblastoma multiforme. Science. 2008; 321:1807–1812.

Patlak CS, Blasberg RG, Fenstermacher JD. Graphical evaluation of blood-to-brain transfer constants from multiple-time uptake data. J Cereb Blood Flow Metab. 1983; 3:1–7.

Pelletier G, Verhoef MJ, Khatri N, Hagen N. Quality of life in brain tumor patients: the relative contributions of depression, fatigue, emotional distress, and existential issues. J Neurooncol. 2002; 57:41–49.

Perry A, Louis DN, Scheithauer BW, Budka H, von Deimling. Meningiomas. In: Louis DN, Ohgaki H, Wiestler OD, Cavenee WK, editors. WHO classification of tumours of the central nervous system. Lyon: IARC press. 2007.

Pignatti F, van den Bent M, Curran D, Debruyne C, Sylvester R, Therasse P, Afra D, Cornu P, Bolla M, Vecht C, Karim AB; European Organization for Research and Treatment of Cancer Brain Tumor Cooperative Group; European Organization for Research and Treatment of Cancer Radiotherapy Cooperative Group. Prognostic factors for survival in adult patients with cerebral low-grade glioma. J Clin Oncol 2002; 20:2076–2084.

Pilotte L, Larrieu P, Stroobant V, Colau D, Dolusic E, Frédérick R, De Plaen E, Uyttenhove C, Wouters J, Masereel B, Van den Eynde BJ. Reversal of tumoral immune resistance by inhibition of tryptophan 2,3-dioxygenase. Proc Natl Acad Sci U S A. 2012; 109:2497–2502.

Porter KR, McCarthy BJ, Freels S, Kim Y, Davis FG. Prevalence estimates for primary brain tumors in the United States by age, gender, behavior, and histology. Neuro Oncol. 2010; 12:520–527.

Posti JP, Bori M, Kauko T, Sankinen M, Nordberg J, Rahi M, Frantzén J, Vuorinen V, Sipilä JO. Presenting symptoms of glioma in adults. Acta Neurol Scand. 2015; 131:88-93.

Rinaldi M, Caffo M, minutoli L, Marini H, Abbritti RV, Squadrito F, Trichilo V, Valenti A, Barresi V, Altavilla D, Passalacqua M, Caruso G. ROS and Brain Gliomas: An Overview of Potential and Innovative Therapeutic Strategies. Int J Mol Sci. 2016; 22; 17

Riva M, Salmaggi A, Marchioni E, Silvani A, Tomei G, Lorusso L, Merli R, Imbesi F, Russo A; Lombardia Neurooncology Group. Tumour-associated epilepsy: clinical impact and the role of referring centres in a cohort of glioblastoma patients. A multicentre study from the lombardia neurooncology group. Neurol Sci. 2006; 27:345–351.

Rogers CL, Perry A, Pugh S, Vogelbaum MA, Brachman D, McMillan W, Jenrette J, Barani I, Shrieve D, Sloan A, Bovi J, Kwok Y, Burri SH, Chao ST, Spalding AC, Anscher MS, Bloom B, Mehta M. Pathology concordance levels for meningioma classification and grading in NRG Oncology RTOG Trial 0539. Neuro Oncol. 2016; 18:565–574.

Rooney AG, McNamara S, Mackinnon M, Fraser M, Rampling R, Carson A, Grant R. Frequency, clinical associations, and longitudinal course of major depressive disorder in adults with cerebral glioma. J Clin Oncol. 2011; 29:4307–4312.

Rooney AG, Carson A, Grant R. Depression in cerebral glioma patients: a systematic review of observational studies. J Natl Cancer Inst. 2011; 103:61–76.

Ruda R, Trevisan E, Soffietti R. Epilepsy and brain tumors. Curr Opin Oncol 2010; 22:611–620.

Ruda R, Bello L, Duffau H, Soffietti R. Seizures in low grade gliomas: natural history, pathogenesis, and outcome after treatments. Neuro Oncol. 2012; 14:iv55–64.

Sahm F, Reuss D, Koelsche C, Capper D, Schittenhelm J, Heim S, Jones DT, Pfister SM, Herold-Mende C, Wick W, Mueller W, Hartmann C, Paulus W, von Deimlimg A. Farewell to oligoastrocytoma: in situ molecular genetics favor classification as either oligodendroglioma or astrocytoma. Acta Neuropathol. 2014; 128:551–559.

Sahm F, Schrimpf D, Olar A, Koelsche C, Reuss D, Bissel J, Kratz A, Capper D, Schefzyk S, Hielscher T, Wang Q, Sulman EP, Adeberg S, Koch A, Okuducu AF, Brehmer S, Schittenhelm J, Becker A, Brokinkel B, Schmidt M, Ull T, Gousias K, Kessler AF, Lamszus K, Debus J, Mawrin C, Kim YJ, Simon M, Ketter R, Paulus W, Aldape KD, Herold-Mende C, von Deimling A. TERT promoter mutations and risk of recurrence in meningioma. J Natl Cancer Inst. 2015; 108:pii:djv377.

Saraf S, McCarthy BJ, Villano JL. Update on Meningiomas. The Oncologist 2011; 16:1604-1613.

Schag CC, Heinrich RL, Ganz PA. Karnofsky performance status revisited: reliability, validity, and guidelines. J Clin Oncol. 1984; 2:187-93.

Schiepers C, Chen W, Cloughesy T, Dahlbom M, Huang SC. ^{18}F-FDOPA kinetics in brain tumors. J Nucl Med. 2007; 48:1651–1661.

Schoemaker MJ, Swerdlow AJ, Hepworth SJ, McKinney PA, van Tongeren M, Muir KR. History of allergies and risk of glioma in adults. Int J Cancer. 2006; 119:2165–2172.

Schouten LJ, Rutten J, Huveneers HA, Twijnstra A. Incidence of brain metastases in a cohort of patients with carcinoma of the breast, colon, kidney, and lung and melanoma. Cancer. 2002; 94:2698-2705.

Schwartzbaum J, Jonsson F, Ahlbom A, Preston-Martin S, Lönn S, Söderberg KC, Feychting M. Cohort studies of association between self-reported allergic conditions, immune-related diagnoses and glioma and meningioma risk. Int J Cancer. 2003; 106:423–428.

Simon R. Clinical trial designs for evaluating the medical utility of prognostic and predictive biomarkers in oncology. Per Med. 2010; 7:33–47.

Simpson D. The recurrence of intracranial meningiomas after surgical treatment. J Neurol Neurosurg Psychiatry. 1957; 20:22−39.

Skjulsvik AJ, Mørk JN, Torp MO, Torp SH. Ki-67/MIB-1 immunostaining in a cohort of human gliomas. Int J Clin Exp Pathol. 2014; 7:8905-8910.

Smith TA. The rate-limiting step for tumor [^{18}F]fluoro-2-deoxy-D-glucose (FDG) incorporation. Nucl Med Biol. 2001; 28:1–4.

Soffietti R, Rudā R, Mutani R. Management of brain metastases. J Neurol. 2002; 249:1357-1369.

Sperduto PW, Kased N, Roberge D, Xu Z, Shanley R, Luo X, Sneed PK, Chao ST, Weil RJ, Suh J, Bhatt A, Jensen AW, Brown PD, Shih HA, Kirkpatrick J, Gaspar LE, Fiveash JB, Chiang V, Knisely JP, Sperduto CM, Lin N, Mehta M. Effect of tumor subtype on survival and the graded prognostic assessment for patients with breast cancer and brain metastases. Int J Radiat Oncol Biol Phys. 2012; 82:2111-7.

Storch EA, Roberti JW, Roth DA. Factor structure, concurrent validity, and internal consistency of the Beck Depression Inventory-Second Edition in a sample of college students. Depress Anxiety. 2004; 19:187–189.

Stupp R, Mason WP, van den Bent MJ, Weller M, Fisher B, Taphoorn MJ, Belanger K, Brandes AA, Marosi C, Bogdahn U, Curschmann J, Janzer RC, Ludwin SK, Gorlia T, Allgeier A, Lacombe D, Cairncross JG, Eisenhauer E, Mirimanoff RO; European Organisation for Research and Treatment of Cancer Brain Tumor and Radiotherapy Groups; National Cancer Institute of Canada Clinical Trials Group. Radiotherapy plus concomitant and adjuvant temozolomide for glioblastoma. N Engl J Med. 2005; 352:987–996.

Stupp R, Hegi ME, Mason WP, van den Bent MJ, Taphoorn MJ, Janzer RC, Ludwin SK, Allgeier A, Fisher B, Belanger K, Hau P, Brandes AA, Gijtenbeek J, Marosi C, Vecht CJ, Mokhtari K, Wesseling P, Villa S, Eisenhauer E, Gorlia T, Weller M, Lacombe D, Cairncross JG, Mirimanoff RO; European Organisation for Research and Treatment of Cancer Brain Tumour and Radiation Oncology Groups; National Cancer Institute of Canada Clinical Trials Group. Effects of radiotherapy with concomitant and adjuvant temozolomide versus radiotherapy alone on survival in glioblastoma in a randomised phase III study: 5-year analysis of the EORTC-NCIC trial. Lancet Oncol. 2009; 10: 459-466.

Stupp R, Wong ET, Kanner AA, Steinberg D, Engelhard H, Heidecke V. NovoTTF-100A versus physician's choice chemotherapy in recurrent glioblastoma: a randomised phase III trial of a novel treatment modality. Eur J Cancer. 2012; 48:2192-2202.

Stupp R, Taillibert S, Kanner AA, Kesari S, Steinberg DM, Toms SA, Taylor LP, Lieberman F, Silvani A, Fink KL, Barnett GH, Zhu JJ, Henson JW, Engelhard HH, Chen TC, Tran DD, Sroubek J, Tran ND, Hottinger AF, Landolfi J, Desai R, Caroli M, Kew Y, Honnorat J, Idbaih A, Kirson ED, Weinberg U, Palti Y, Hegi ME, Ram Z. Maintenance Therapy With Tumor-Treating Fields Plus Temozolomide vs Temozolomide Alone for Glioblastoma: A Randomized Clinical Trial. JAMA. 2015; 314:2535-2543.

Surveillance Epidemiology and End Results (SEER) Program. SEER*Stat database: Incidence-SEER 18 Regs Research Data + Hurricane Katrina Impacted Louisiana Cases, Nov 2015 Sub (1973-2013 varying)-Linked to County Attributes-Total U.S., 1969-2014 Counties, National cancer Institute, DCCPS, Surveillance Research Program,

Surveillance System Branch, released April 2016, based on the November 2015 submission.

Takeguchi T, Miki H, Shimizu T, Kikuchi K, Mochizuki T, Ohue S, Ohnishi T. The dural tail of intracranial meningiomas on fluid-attenuated inversion-recovery images. Neuroradiology. 2004; 46:130−135.

Tanaka S, Meyer F, Buckner J, Uhm J, Yan E, Parney I. Presentation, management, and outcome of elderly patients with newly-diagnosed anaplastic astrocytoma. J Neurooncol 2012; 110:227–235.

Tashiro M, Juengling FD, Reinhardt MJ, Brink I, Hoegerle S, Mix M, Kubota K, Yamaguchi K, Itoh M, Sasaki H, Moser E, Nitzsche EU. Reproducibility of PET brain mapping of cancer patients. Psycho-oncology. 2000; 9:157–163.

Tashiro M, Juengling FD, Reinhardt MJ, Mix M, Kumano H, Kubota K, Itoh M, Sasaki H, Nitzsche EU, Moser E. Depressive state and regional cerebral activity in cancer patients - a preliminary study. Med Sci Monit. 2001; 7:687–695.

Tezak Z, Kondratovich MV, Mansfield E. US FDA and personalized medicine: in vitro diagnostic regulatory perspective. Per Med. 2010; 7:517–530.

Uyttenhove C, Pilotte L, Théate I, Stroobant V, Colau D, Parmentier N, Boon T, Van den Eynde BJ. Evidence for a tumoral immune resistance mechanism based on tryptophan degradation by indoleamine 2,3-dioxygenase. Nat Med. 2003; 9:1269-1274.

van Waarde A, Elsinga PH. Proliferation markers for the differential diagnosis of tumor and inflammation. Curr Pharm Des. 2008; 14:3326–3339.

Venur VA, Ahluwalia MS. Prognostic scores for brain metastases patients: use in clinical practice a d trial design. Chin Clin Oncol. 2015; 4:18.

Verhaak RG, Hoadley KA, Purdom E, Wang V, Qi Y, Wilkerson MD, Miller CR, Ding L, Golub T, Mesirov JP, Alexe G, Lawrence M, O'Kelly M, Tamayo P, Weir BA, Gabriel S, Winckler W, Gupta S, Jakkula L, Feiler HS, Hodgson JG, James CD, Sarkaria JN, Brennan C, Kahn A, Spellman PT, Wilson RK, Speed TP, Gray JW, Meyerson M, Getz G, Perou CM, Hayes DN; Cancer Genome Atlas Research Network. Integrated genomic analysis identifies clinically relevant subtypes of glioblastoma characterized by abnormalities in PDGFRA, IDH1, EGFR, and NF1. Cancer Cell. 2010; 17:98-110.

Vredenburgh JJ, Desjardins A, Herndon JE 2nd, Marcello J, Reardon DA, Quinn JA, Rich JN, Sathornsumetee S, Gururangan S, Sampson J, Wagner M, Bailey L, Bigner DD, Friedman AH, Friedman HS. Bevacizumab plus irinotecan in recurrent glioblastoma multiforme. J Clin Oncol. 2007; 25:4722–4729.

Wang J, Cazzato E, Ladewig E, Frattini V, Rosenbloom DI, Zairis S, Abate F, Liu Z, Elliott O, Shin YJ, Lee JK, Lee IH, Park WY, Eoli M, Blumberg AJ, Lasorella A, Nam DH, Finocchiaro G, Iavarone A, Rabadan R. Clonal evolution of glioblastoma under therapy. Nat Genet. 2016; 48:768-776.

Weller M, Yung WK. Angiogenesis inhibition for glioblastoma at the edge: beyond AVAGlio and RTOG 0825. Neuro Oncol. 2013; 15:971.

Wen PY, Kesari S. Malignant gliomas in adults. N Engl J Med. 2008; 359:492-507.

Wester HJ, Herz M, Weber W, Heiss P, Senekowitsch-Schmidtke R, Schwaiger M, Stöcklin G. Synthesis and radiopharmacology of O-(2-[^{18}F]fluoroethyl)-L-tyrosine for tumor imaging. J Nucl Med. 1999; 40:205–212.

Wiemels JL, Wiencke JK, Sison JD, Miike R, McMillan A, Wrensch M. History of allergies among adults with glioma and controls. Int J Cancer. 2002; 98:609–615.

Wiestler B, Capper D, Sill M, Jones DT, Hovestadt V, Sturm D, Koelsche C, Bertoni A, Schweizer L, Korshunov A, Weiß EK, Schliesser MG, Radbruch A, Herold-Mende C, Roth P, Unterberg A, Hartmann C, Pietsch T, Reifenberger G, Lichter P, Radlwimmer B, Platten M, Pfister SM, von Deimling A, Weller M, Wick W. Integrated DNA methylation and copy-number profiling identify three clinically and biologically relevant groups of anaplastic glioma. Acta Neuropathol. 2014; 128:561–571.

Wilson TA, Karajannis MA, Harter DH. Glioblastoma multiforme: State of the art and future therapeutics. Surg Neurol Int. 2014; 8:64.

Winther TL, Torp SH. The significance of the extent of resection in modern neurosurgical practice of WHO grade I meningiomas. World Neurosurg. 2016.pii:31182-2.

Wong J, Hird A, Kirou-Mauro A, Napolskikh J, Chow E. Quality of life in brain metastases radiation trials: a literature review. Curr Oncol. 2008; 15:25-45.

Wong E, Rowbottom L, Tsao M, Zhang L, McDonald R, Danjoux C, Barnes E, Chan S, Chow E. Correlating symptoms and their changes with survival in patients with brain metastases. Ann Palliat Med. 2016; 5:253-266.

Wöhrer A, Waldhör T, Heinzl H, Hackl M, Feichtinger J, Gruber-Mösenbacher U, Kiefer A, Maier H, Motz R, Reiner-Concin A, Richling B, Idriceanu C, Scarpatetti M, Sedivy R, Bankl HC, Stiglbauer W, Preusser M, Rössler K, Hainfellner JA. The Austrian Barin Tumour Registry: a cooperative way to establish a population-based brain tumour registry. J Neurooncol. 2009; 95:401-411.

Xin Y, Cai H. Improved Radiosynthesis and Biological Evaluations of L- and D-1-[^{18}F]Fluoroethyl-Tryptophan for PET Imaging of IDO-Mediated Kynurenine Pathway of Tryptophan Metabolism. Mol Imaging Biol. 2017; 19:589-598.

Yoo MY, Paeng JC, Cheon GJ, Lee DS, Chung JK, Kim EE, Kang KW. Prognostic Value of Metabolic Tumor Volume on ^{11}C-Methionine PET in Predicting Progression-Free Survival in High-Grade Glioma. Nucl Med Mol Imaging. 2015; 49:291-297.

Young GS. Advanced MRI of adult brain tumors. Neurol Clin. 2007; 25:947-973.

Yuan Y, Qi C, Maling G, Xiang W, Yanhui L, Ruofei L, Yunhe M, Jiewen L, Qing M. TERT mutation in glioma: Frequency, prognosis and risk. J Clin Neurosci. 2016; 26:57-62.

Zhang H, Rödiger LA, Shen T, Miao J, Oudkerk M. Preoperative subtyping of meningiomas by perfusion MR imaging. Neuroradiology. 2008; 50:835−840.

Zinn PO, Colen RR. Imaging genomic mapping in glioblastoma. Neurosurgery. 2013; 60:126–130.

Zitron IM, Kamson DO, Kiousis S, Juhász C, Mittal S. In vivo metabolism of tryptophan in meningiomas is mediated by indoleamine 2,3-dioxygenase 1. Cancer Biol Ther. 2013; 14:333–339.

VIII. LIST OF PUBLICATIONS

VIII.1. Peer-reviewed publications related to this thesis

1. **Bosnyák** E, Kamson DO, Guastella AR, Varadarajan K, Robinette NL, Kupsky WJ, Muzik O, Michelhaugh SK, Mittal S, Juhász C. Molecular imaging correlates of tryptophan metabolism via the kynurenine pathway in human meningiomas. Neuro Oncol. 2015; 17:1284-92. (**IF 7.37**)

2. **Bosnyák** E, Kamson DO, Behen ME, Barger GR, Mittal S, Juhász C. Imaging cerebral tryptophan metabolism in brain tumor-associated depression. EJNMMI Res. 2015; 5:56. (**IF: 1.761**)

3. **Bosnyák** E, Kamson DO, Robinette NL, Barger GR, Mittal S, Juhász C. Tryptophan PET predicts spatial and temporal patterns of post-treatment glioblastoma progression detected by contrast-enhanced MRI. J Neurooncol. 2016; 126:317-25. (**IF: 2.754**)

4. **Bosnyák** E, Michelhaugh SK, Klinger NV, Kamson DO, Barger GR, Mittal S, Juhász C. Prognostic Molecular and Imaging Biomarkers in Primary Glioblastoma. Clin Nucl Med, 2017; 42:341-7. (**IF: 4.563**)

5. Juhász C, **Bosnyák** E. PET and SPECT studies in children with hemispheric low-grade gliomas. Childs Nerv Syst. 2016; 32:1823-32. (**IF: 1.08**)

6. Erdélyi-Bótor S, Komáromy H, Kamson DO, Kovács N, Perlaki G, Orsi G, Molnár T, Illes Z, Nagy L, Kéki S, Deli G, **Bosnyák** E, Trauninger A, Pfund Z. Serum L-arginine and dimethylarginine levels in migraine patients with brain white matter lesions. Cephalalgia. 2017; 37:571-580. (**IF: 6.05**)

7. Jeong JW, Juhász C, Mittal S, **Bosnyák** E, Kamson DO, Barger GR, Robinette NL, Kupsky WJ, Chugani DC. Multi-modal imaging of tumor cellularity and tryptophan metabolism in human gliomas. Cancer Imaging. 2015; 15:10. (**IF: 1.47**)

8. **Bosnyák** E, Barger GR, Michelhaugh S, Robinette NL, Amit-Yousif A, Mittal S, Juhász C. Amino Acid PET Imaging of the Early Metabolic Response during Tumor-Treating Fields (TTFields) Therapy in Recurrent Glioblastoma. Clin Nucl Med. 2018; 43:176-179. (**IF: 4.563**)

VIII.2. Peer-reviewed publications not related to this thesis

1. **Bosnyák** E, Behen ME, Guy WC, Asano E, Chugani HT, Juhász C. Predictors of Cognitive Functions in Children With Sturge-Weber Syndrome: A Longitudinal Study. Pediatr Neurol. 2016; 61:38-45. (**IF: 1.866**)

2. **Bosnyák E**, Herceg M, Pál E, Aschermann Z, Janszky J, Késmárki I, Komoly S, Karádi K, Dóczi T, Nagy F, Kovács N. Are branded and generic extended-release ropinirole formulations equally efficacious? A rater-blinded, switch-over, multicenter study. Parkinsons Dis. 2014; 2014:158353. (**IF: 2.01**)

3. Deli G, **Bosnyak E**, Pusch G, Komoly S, Feher G. Diabetic Neuropathies: Diagnosis and Management. Neuroendocrinology. 2014, Vol.98,No.4. (**IF: 4.373**)

4. Karádi K, Lucza T, Aschermann Z, Komoly S, Deli G, **Bosnyák E**, Acs P, Horváth R, Janszky J, Kovács N. Visuospatial impairment in Parkinson's disease: the role of laterality. Laterality. 2015; 20:112-27. **(IF: 1.312**)

5. Szapary L, Fehér G, **Bosnyák E**, Deli G, Csécsei P. Effective, safe stroke prevention with novel oral anticoagulants in patients with atrial fibrillation. Focus on dabigatran. Ideggy Sz. 2013; 66: 165-74. (**IF: 0.343**)

6. Deli G, Balás I, Komoly S, Dóczi T, Janszky J, Illés Z, Aschermann Z, Tasnádi E, Nagy F, Pfund Z, Bóné B, **Bosnyák E**, Kuliffay Z, Szijjartó G, Kovács N. Treatment of dystonia by deep brain stimulation: a summary of 40 cases. Ideggy Sz. 2012; 65:249-60. (**IF: 0.348**)

7. Toth P, KoIler A, Pusch G, **Bosnyak E**, Szapary L, Komoly S, et al. Microalbuminuria, indicated by total versus immunoreactive urinary albumins, in acute ischemic stroke patients. J Stroke Cerebrovasc Dis. 2011; 20:510-6. (**IF: 1.68**)

8. Deli G, Balás I, Komoly S, Dóczi T, Janszky József, Aschermann Z, Nagy F, **Bosnyák E**, Kovács N. Earlier and more efficiently: The role of Deep Brain Stimulation in Parkinson's Disease: preserving the working capability. Ideggyogy Sz. 2015; 68:384-90. (**IF: 0.376**)

9. Horváth K, Aschermann Z, Ács P, **Bosnyák E**, Deli G, et al. Validation of the Hungarian Unified Dyskinesia Rating Scale. Ideggyogy Sz. 2015; 68:183-8. (**IF: 0.376**)

10. Deli G, Aschermann Z, Ács P, **Bosnyák E**, Janszky J, et al. Bilateral Subthalamic Stimulation can Improve Sleep Quality in Parkinson's Disease. J Parkinsons Dis. 2015; 5:361-8. (**IF: 3.015**)

11. Kovács N, Aschermann Z, Ács P, **Bosnyák E**, Deli G, Janszky J, Komoly S. The impact of levodopa-carbidopa intestinal gel on health-related quality of life in Parkinson's disease. Ideggyogy Sz. 2014; 67:245-50. (**IF: 0.386**)

12. Horváth K, Aschermann Z, Acs P, **Bosnyák E**, Deli G, et al. Is the MDS-UPDRS a Good Screening Tool for Detecting Sleep Problems and Daytime Sleepiness in Parkinson's Disease? Parkinsons Dis. 2014; 2014:806169. (**IF: 2.01**)

VIII.3. Presentations related to this thesis

Bosnyák E, Kamson D, Muzik O, Mittal S, Juhász C. Characterization of meningiomas by kinetic analysis of alpha[C-11]-methyl-L-tryptophan PET. Presented at the 21st Annual Meeting of the Organization for Human Brain Mapping, Honolulu, HI, June 14-18, 2015.

Bosnyák E, Kamson D, Behen M, Barger G, Mittal S, Juhász C. Correlation of cerebral tryptophan metabolism with brain tumor-associated depression: A PET study. Presented at the 21st Annual Meeting of the Organization for Human Brain Mapping, Honolulu, HI, June 14-18, 2015.

Bosnyák E, Kamson D, Robinette N, Barger G, Mittal S, Juhász C. Multimodal imaging of spatial patterns of post-treatment glioblastoma progression. Neuro-Oncology 2015; 17(suppl 5):v162. doi:10.1093/neuonc/nov225.38. Presented at the 20th Annual Scientific Meeting of the Society for Neuro-Oncology, San Antonio, TX, November 19-22, 2015.

Juhász C, **Bosnyák E**, Kamson D, Barger G, Behen M, Mittal S. Imaging cerebral tryptophan metabolism in brain tumor-associated depression. Neuro-Oncology 2015; 17 (suppl 5): v162. doi: 10.1093/neuonc/nov225.37. Presented at the 20th Annual Scientific Meeting of the Society for Neuro-Oncology, San Antonio, TX, November 19-22, 2015.

Bosnyák E, Michelhaugh SK, Klinger NV, Barger GR, Mittal S, Juhász C. Amino acid metabolism measured by PET is associated with specific molecular biomarkers in primary gliobastoma. Neuro-Oncology 2016; 18(suppl 6): vi132. Presented at the 21st Annual Scientific Meeting of the Society for Neuro-Oncology, Scottsdale, AZ, November 17-21, 2016.

Juhász C, Mittal S, Shah VB, **Bosnyák E**, Barger GR. Imaging the early metabolic response during tumor-treating fields therapy in recurrent glioblastoma. Neuro-Oncology 2016; 18(Suppl 6): vi132. Presented at the 21st Annual Scientific Meeting of the Society for Neuro-Oncology, Scottsdale, AZ, November 17-21, 2016.

Bosnyák E, John F, Robinette NL, Yousif A, Barger GR, Mittal S, Juhász C. Amino acid PET and perfusion MRI in contrast-enhancing and non-enhancing regions of glioblastomas. Neuro-Oncology, 2017; 19(suppl 6): vi161. Presented at the 22nd Annual Scientific Meeting of the Society for Neuro-Oncology, San Francisco, CA, November 16-19, 2017.

IX. ACKNOWLEDGEMENT

My studies were supported by research grants from the National Cancer Institute (R01 CA123451) and from the National Institute of Neurological Disorders and Stroke (R01 NS04192222). Tissue sections were prepared by the Biobanking and Correlative Sciences Core, which is supported in part by National Institutes of Health Center Grant P30 CA022453 to the Karmanos Cancer Institute at Wayne State University (WSU).

My work could not have been carried out without the help of many people, to whom I am really grateful:

First of all, I would like to thank to my supervisor, Professor Csaba Juhász for supporting me, teaching me the basics of neuroimaging in neuro-oncology, especially AMT-PET, and for his continuous support during my years at WSU, and also for his advise in summarizing my thesis.

I also thank to my co-mentor, Dr. Zoltán Pfund for supporting my trip to the US, encouraging me during those years, and advising me with my work on my thesis.

I am grateful to Professor Sámuel Komoly and Professor József Janszky, who also supported me when I got this opportunity.

I would like to say a big thank you to all those colleagues and staff who supported my work at Wayne State University:

Prof. Sandeep Mittal, MD (Chair, Neurosurgery), and Geoffrey Barger, MD (Neurology), Co-directors of the WSU/Karmanos Cancer Institute Neuro-Oncology Multidisciplinary Team; Natasha L. Robinette, MD, and Alit Yousif, MD (Radiology), for reviewing the clinical MRI scans; Thomas Mangner, PhD (PET Center, Children's Hospital of Michigan) for performing AMT radiochemistry; Cathie Germain, MA, Cynthia Burnett, BA, and Kelly Forcucci, RN, for assisting patient recruitment and scheduling; and Ms. Lynda Ferguson, for her continuous support in human subjects research administration.

I also thank James Janisse, PhD, for assisting with the statistical analysis, and Sharon Michelhaugh, PhD, who supervised tumor tissue studies at the WSU Neuro-Oncology Research Laboratory.

I am very grateful to the entire staff at the PET Center, Children's Hospital of Michigan, who provided invaluable technical help in performing the PET scans and for constantly advising and helping me.

Special thanks to all of my friends in the US and Hungary for their continuous support.

Finally, I would like to express my gratitude to my parents, my sisters, and my grandmother for their love and for supporting and encouraging me through all these years.

Leaving them behind and living in the US was a big decision, but one of the best ones in my life. My family always supported and stood by me in this endaveour, and I cannot be grateful enough to them.